Journal of Saudi Chemical Society (2016) **20**, S357–S375

King Saud University

Journal of Saudi Chemical Society

www.ksu.edu.sa
www.sciencedirect.com

ORIGINAL ARTICLE

Kinetic and mechanistic investigations of chlorocomplex of Ru(III) and Ir(III) catalyzed oxidation of D-fructose by N-bromophthalimide in acidic medium

Neerja Sachdev [a], Ajaya Kumar Singh [b,*], Alpa Shrivastava [c], Yokraj Katre [d]

[a] *Department of Applied Chemistry, Bhilai School of Engineering, Durg, India*
[b] *Department of Chemistry, Govt. V.Y.T.PG. Autonomous College, Durg (C.G.), India*
[c] *Department of Applied Chemistry, Shri Shankaracharya Group of Institute, Bhilai, India*
[d] *Department of Chemistry, Kalyan Mahavidyalaya, Bhilai Nagar Sect-7, Bhilai, India*

Received 15 September 2012; accepted 9 December 2012
Available online 28 December 2012

KEYWORDS

Kinetics;
Oxidation;
N-bromophthalimide (NBP);
D-fructose (D-fru);
Ru(III) chloride;
Ir(III) chloride;
Phthalimide (NHP)

Abstract The kinetic and mechanistic studies of Ru(III) and Ir(III) homogeneously catalyzed oxidation of D-fructose (D-fru) by N-bromophthalimide (NBP) in the presence of aqueous perchloric acid medium have been made at 303 K using mercuric acetate as Br^- ion scavenger. The stoichiometry and the oxidation products in both catalysts were found to be the same. The determined stoichiometric ratio was found to be 1:2 ([D-fru]:[NBP]). Arabinonic and formic acids were obtained as the major oxidized products of both the reactions. The kinetics of the reaction were studied as a function of temperature, ionic strength, concentration of the salt, concentration of the added reaction product, and the dielectric constant of the medium to learn the mechanistic aspects of the reaction. Possible mechanisms are proposed, which are consistent with the kinetics, stoichiometry and products of the reaction.

1. Introduction

In the modern chemical industries, increasing requirement of catalyst selectivity has become an issue of growing concern. However, in the studies of active center structure by means of physical method, the reaction pathway regarding complicated molecules cannot be calculated. The reaction mechanism of various elementary reactions must be investigated to analyze the factors affecting selectivity (Kong et al., 2002). Transition metals in higher oxidation states can generally be stabilized by chelation with suitable complexing agents (Zhai et al., 2007). Therefore, the basic studies of catalytic reactions will provide the scientific basis for improving catalyst' selectivity and producing high-efficiency catalysts. The use of transition metal ions either alone or as binary mixtures as catalysts has received much interest in many redox reactions. Their oxidizing and

* Corresponding author. Tel.: +91 788 2223421; fax: +91 788 2212030.
E-mail address: ajayaksingh_au@yahoo.co.in (A.K. Singh).

Peer review under responsibility of King Saud University.

Production and hosting by Elsevier

http://dx.doi.org/10.1016/j.jscs.2012.12.006

catalytic activities are due to the existence of variable oxidation states, as a consequence of partly filled d or f orbitals. Their ability to form both sigma and π bonds with other moieties or legends is one of the chief factors for importing catalytic properties to transition metal ion as well as their complexes (Singh et al., 2008). Among the different metal ions, Ru(III) and Ir(III) are highly efficient (Singh et al., 2009a). Though Ru(III) is a known nontoxic homogenous catalyst, scant attention has been paid to explore the catalytic role of Ru (III) with N-halo compounds as oxidant (Singh et al., 2009b,c). Ru(III) is an efficient catalyst in several redox reactions (Singh et al., 2009d). The potential of Ir(III) chloride to act as homogeneous catalyst in the oxidation process was also recognized by various workers (Mohanty et al., 1998; Das, 1996; Das and Das, 1995; Singh et al., 2004, 2009, 2012).

Several studies have been reported to explore the wide range of properties of N-halo compounds (Chandra and Srivastava, 1972; Rao et al., 1979; Kantouch and Fattah, 1971). N-halo compounds have extensively been used as an oxidizing agent for the catalyzed and uncatalyzed reactions (Singh et al., 1988, 2002, 2003, 2006a, 2006b; Khanchandani et al., 1996; Chaudhary et al., 1999; Vyas and Sharma, 2001; Kumbhat et al., 2002; Katre et al., 2012a, 2012b, 2012c, 2012d). Because of the biochemical importance of D-fru in metabolic system, its physico-chemical properties in solution have been extensively studied (White et al., 1959; Doty and Wannien, 1975). Several reports are also available in the literature for the oxidation of D-fru (Das et al., 2001) by NBP. Vast literature is available on the kinetics of oxidation of carbohydrates by various organic and inorganic oxidants (Malik et al., 2009; Singh et al., 2007a). Transition metal catalyzed reactions have also created a great interest, due to their involvement in many important industrial processes, such as hydrogenation, carbonylation reactions and low pressure polymerization of ethylene and propene (Singh et al., 2007b; Cotton et al., 1999). Lack of studies on the oxidation of D-fru by NBP in acidic medium in the presence of Ir(III) and Ru(III) has encouraged us to investigate the kinetic behavior of the title reaction in order to continue our study on the role of metal ions in oxidation reactions by NBP. In the present study we are reporting the detailed kinetics of the Ru(III) as well as Ir(III) catalyzed oxidation of D-fru in acidic medium with a view to ascertain the active species, to know the comparative catalytic efficiency of Ru(III) and Ir(III) and to find out mechanistic aspects of the reactions.

2. Experimental

2.1. Material and method

A stock standard solution of NBP (E. Merck) was prepared by dissolving its known weight in 50% acetic acid and its concentration was estimated iodometrically. In order to avoid photochemical deterioration, the solution of NBP was preserved in black coated flask. The standard solution of D-fru (AR Grade) was freshly prepared. Stock solutions of Ru(III) chloride (Johnson-Matthey) and Ir(III) chloride (Johnson-Matthey) were prepared by dissolving in HCl of known strength. The Ru(III) concentration was assayed by EDTA titration (Reddy and Kumar, 1995) and also both catalysts were stored in a black coated bottle to prevent photochemical decomposition. Other reagents used were of AR grade and their solutions were also prepared in doubly distilled water.

All the kinetic measurements were carried out in a black-coated vessel at a constant temperature, 303 K and performed under pseudo first order condition with [D-fru] ≫ [NBP]. The reaction was initiated by mixing the already thermo-stated solution of D-fru to the thermally equilibrated reaction mixture containing required volumes of solutions of NBP, H^+, Ru(III) or Ir(III) and all other reagents. Aliquots (2 ml) of the reaction mixture were pipetted out at regular intervals of time and poured into a conical flask containing 2 ml of 4% KI solution and 2 ml of dilute perchloric acid solution. The liberated iodine equivalent to unconsumed NBP was estimated with a standard sodium-thiosulphate solution using starch as an indicator. Each kinetic run was studied for about 80% of the reaction. The rate constant in each kinetic run was determined by plotting a graph between log [a-x] versus time. Each kinetic run was studied for two half-lives of the reaction. The observed rates of reaction were within ±5% in replicate kinetics runs. The order of reaction in each reactant was determined with the help of log–log plot of k_{obs} versus concentration of reactant.

2.2. Determination of Stoichiometry and Product Analysis

Different ratios of NBP to D-fru (Table 6a and b) were equilibrated at 303 K in the presence of a requisite amount of all reactants i.e. perchloric acid, mercuric acetate and acetic acid under the condition of [NBP] ≫ [D-fru] for 48 h. Determination of unconsumed NBP revealed that two moles of NBP were required for the oxidation of each mole of D-fru as in the following equation.

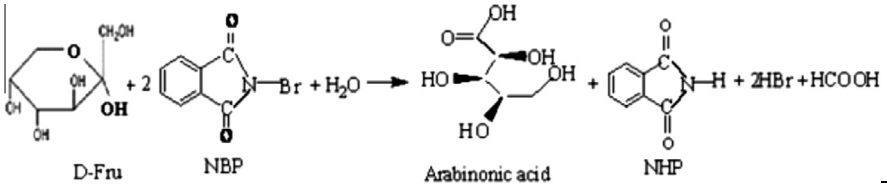

(A)

The reaction products were extracted with ether after completion of the reaction (monitored by TLC). Evaporation of the ether layer was followed by column chromatography on silica gel (60–200 mesh) using a gradient elution (from dichloromethane to chloroform). After the initial separation, the products were further purified by recrystallization. The products were found to be identical under both stoichiometric and kinetic conditions. Identification of major reaction product i.e. arabinonic acid, in the presence of Ru(III) chloride and Ir(III) chloride was confirmed by paper chromatography (Lyengar et al., 1990) and TLC and spot test (Feigl, 1975; Vogel, 1958).

The FTIR spectra (obtained using model No. 8400S, Shimadzu) of the main product showed a sharp band at 1690–1760 (due to C═O stretching) and at 1080–1300 (due to C–O stretching), suggesting the formation of carboxylic acid i.e. Formic acid and Arabinonic acid. The strong broad peaks in the ranges of 3200–3600 indicated the presence of hydrogen bonded alcohols in arabinonic acid. It (3300–3500 stretching) also showed the presence of amines (N–H) i.e. phthalimide (NHP). A band observed at 1600 suggested the aromatic ring in phthalimide.

Finally, the formation of these products was confirmed by GC–MS analysis in which the reaction mixture was extracted with diethyl ether. The ether layer was concentrated by slow evaporation before an analysis by GC–MS, JEOL-JMS (Mate-MS system, Japan). NHP, i.e., the reduced product of NBP was also identified by GC–MS.

3. Results and discussion

Initially, the kinetics of the oxidation of D-fru by NBP in the presence of Ru(III) or Ir(III) under acidic conditions were studied at several initial concentrations of all the reactants at 303 K. Considering NBP, D-fru, hydrogen ions and Ru(III) or Ir(III) as the main reactants, the general form of rate equation for the reaction can be written as

$$\text{rate} = k_{cal}[\text{NBP}]^{\alpha}[\text{D-Fru}]^{\beta}[\text{Ru(III)}]^{\gamma}[\text{H}^{+}]^{\delta} \quad \text{(B)}$$

$$\text{rate} = \boldsymbol{k}_{cal}[\text{NBP}]^{\alpha}[\text{D-Fru}]^{\beta}[\text{Ru(III)}]^{\gamma}[\text{H}^{+}]^{\delta} \quad \text{(C)}$$

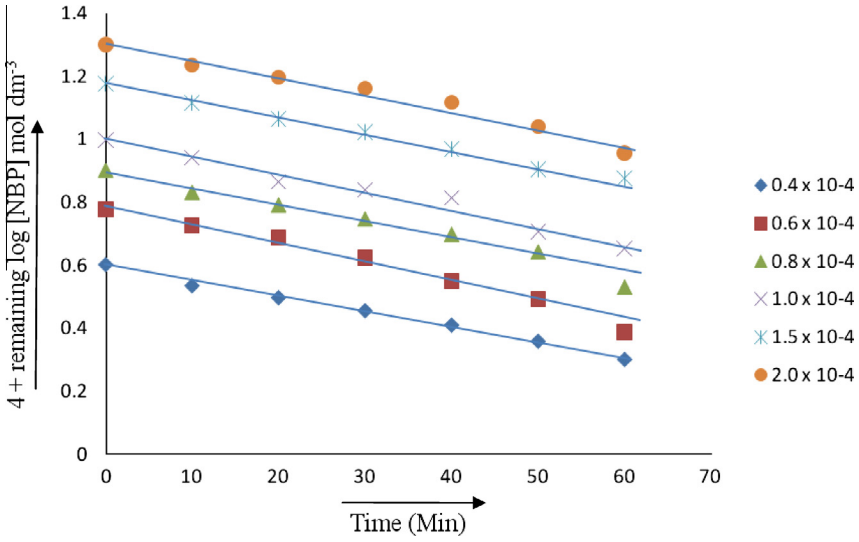

Figure 1 Sample individual time plots for log[NBP] for various concentrations at T = 303 K. (a) [NBP] = 2.00×10^{-4} mol dm^{-3}, [D-fru] = 2.00×10^{-3} mol dm^{-3}, [H^+] = 4.00×10^{-3} mol dm^{-3}, [Ru(III)] = 1.92×10^{-5} mol dm^{-3}, [KCl] = 1.00×10^{-5} mol dm^{-3}, [$Hg(OAc)_2$] = 3.00×10^{-4} mol dm^{-3}, [NHP] = 1.00×10^{-4} mol dm^{-3} and CH_3COOH = 20%. Where a = Ru(III) catalysis.

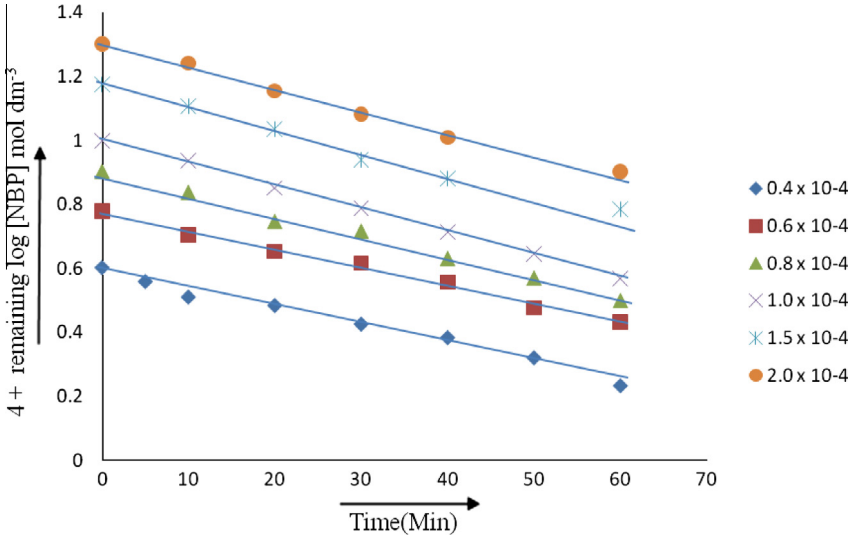

Figure 2 Sample individual time plots for log [NBP] for various concentrations at T = 303 K. (b) [NBP] = 2.00×10^{-4} mol dm^{-3}, [D-fru] = 2.00×10^{-3} mol dm^{-3}, [H^+] = 4.00×10^{-3} mol dm^{-3}, [Ir(III)] = 1.33×10^{-5} mol dm^{-3}, [KCl] = 1.00×10^{-5} mol dm^{-3}, [$Hg(OAc)_2$] = 3.00×10^{-4} mol dm^{-3} and CH_3COOH = 20%. Where b = Ir(III) catalysis.

Table 1 Effect of variation [NBP], [D-fru] and [H^+] on the rate of oxidation of D-fru at 303 K.

[NBP] $\times 10^4$ mol dm^{-3}	[D-fru] $\times 10^3$ mol dm^{-3}	[H^+] $\times 10^3$ mol dm^{-3}	$k_{obs} \times 10^4$ s^{-1} [a]	$k_{obs} \times 10^4$ s^{-1} [b]
0.40	2.00	4.00	2.01	2.56
0.60	2.00	4.00	2.07	2.41
0.80	2.00	4.00	2.17	2.54
1.00	2.00	4.00	2.19	2.62
1.50	2.00	4.00	2.05	2.65
2.00	2.00	4.00	2.08	2.62
2.00	2.00	4.00	2.13	2.50
2.00	3.00	4.00	2.44	2.56
2.00	4.00	4.00	2.25	2.53
2.00	5.00	4.00	1.94	2.50
2.00	6.00	4.00	2.02	2.60
2.00	8.00	4.00	2.12	–
2.00	10.00	4.00	1.69	2.62
2.00	15.00	4.00	–	2.78
2.00	20.00	4.00	–	2.47
2.00	2.00	1.00	0.60	0.51
2.00	2.00	2.00	1.20	0.90
2.00	2.00	3.00	1.56	1.30
2.00	2.00	4.00	2.19	2.20
2.00	2.00	5.00	2.46	2.60
2.00	2.00	8.00	2.76	3.40
2.00	2.00	10.00	3.00	3.90

Solution conditions: (a) [NBP] = 2.00×10^{-4} mol dm^{-3}, [D-fru] = 2.00×10^{-3} mol dm^{-3}, [H^+] = 4.00×10^{-3} mol dm^{-3}, [$Hg(OAc)_2$] = 3.00×10^{-4} mol dm^{-3}, [Ru(III)] = 1.92×10^{-5} mol dm^{-3}, [NHP] = 1.00×10^{-4} mol dm^{-3} [KCl] = 1.00×10^{-5} mol dm^{-3} and CH_3COOH = 20%. (b) [NBP] = 2.00×10^{-4} mol dm^{-3}, [D-fru] = 2.00×10^{-3} mol dm^{-3}, [H^+] = 4.00×10^{-3} mol dm^{-3}, [$Hg(OAc)_2$] = 3.00×10^{-4} mol dm^{-3}, [Ir(III)] = 1.33×10^{-5} mol dm^{-3}, [KCl] = 1.00×10^{-5} mol dm^{-3} and CH_3COOH = 20%. Where, a = Ru(III) catalyzed, b = Ir(III) catalyzed.

[a] Ru(III)catalysis.

[b] Ir(III) catalysis.

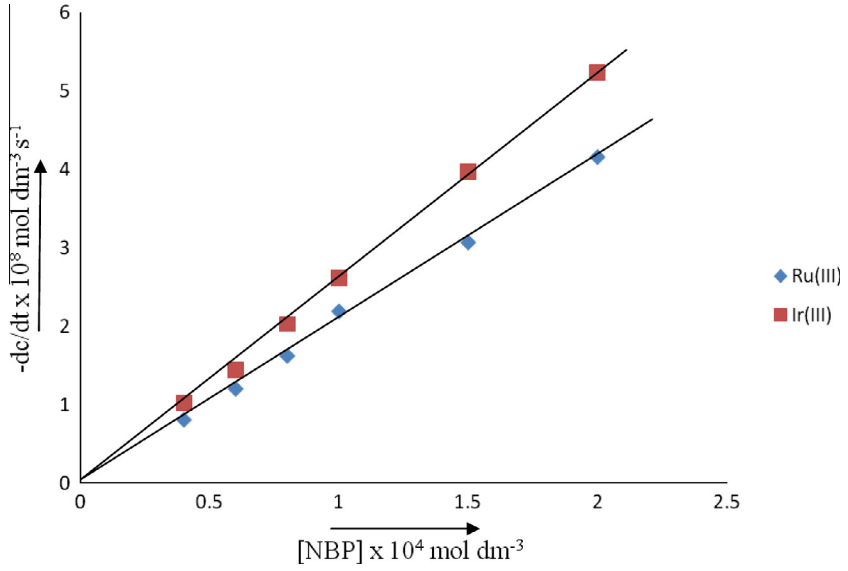

Figure 3 Plot between −dc/dt versus [NBP] at T = 303 K. (a) [NBP] = 2.00×10^{-4} mol dm^{-3}, [D-fru] = 2.00×10^{-3} mol dm^{-3}, [H^+] = 4.00×10^{-3} mol dm^{-3}, [Ru(III)] = 1.92×10^{-5} mol dm^{-3}, [KCl] = 1.00×10^{-5} mol dm^{-3}, [NHP] = 1.00×10^{-4} mol dm^{-3} [$Hg(OAc)_2$] = 3.00×10^{-4} mol dm^{-3} and CH_3COOH = 20%. (b) [NBP] = 2.00×10^{-4} mol dm^{-3}, [D-fru] = 2.00×10^{-3} mol dm^{-3}, [H^+] = 4.00×10^{-3} mol dm^{-3}, [Ir(III)] = 1.33×10^{-5} mol dm^{-3}, [KCl] = 1.00×10^{-5} mol dm^{-3}, [$Hg(OAc)_2$] = 3.00×10^{-4} mol dm^{-3} and CH_3COOH = 20%. Where a = Ru(III) catalysis, b = Ir(III) catalysis.

The rate constant of the reaction in each kinetic run was determined by a plot of the log [NBP] versus time (Figs. 1 and 2), which produced a straight line and indicates that the reaction under the chosen condition follows pseudo first order kinetics (Table 1).

3.1. Kinetics of oxidation of D-fru by NBP in the presence of Ru(III)

The values of rate (−dc/dt) at various concentrations of [NBP] (from 0.40×10^{-4} mol dm^{-3} to 2.00×10^{-4} mol dm^{-3}) clearly

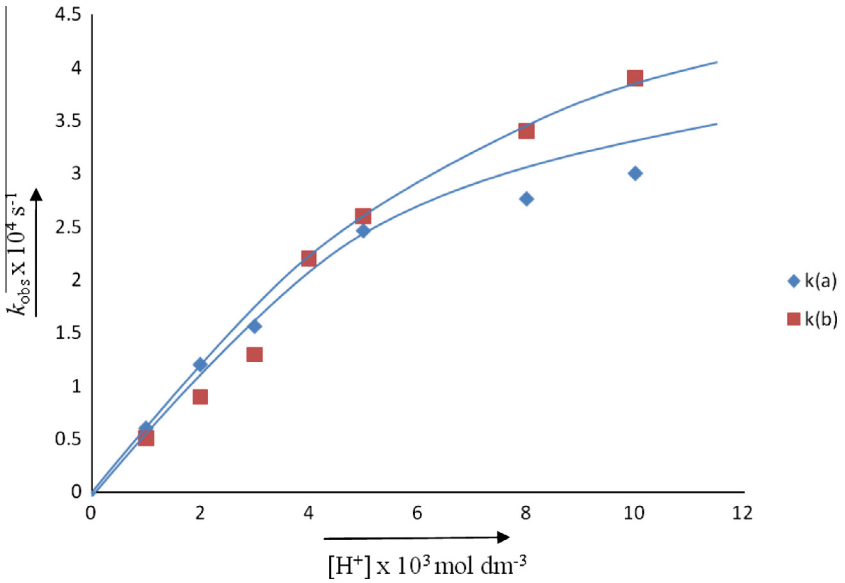

Figure 4 Plot between k_{obs} versus $[H^+]$ at T = 303 K. (a) [NBP] = 2.00×10^{-4} mol dm^{-3}, [D-fru] = 2.00×10^{-3} mol dm^{-3}, $[H^+]$ = 4.00×10^{-3} mol dm^{-3}, [Ru(III)] = 1.92×10^{-5} mol dm^{-3}, [KCl] = 1.00×10^{-5} mol dm^{-3}, [NHP] = 1.00×10^{-4} mol dm^{-3} [$Hg(OAc)_2$] = 3.00×10^{-4} mol dm^{-3} and CH_3COOH = 20%. b [NBP] = 2.00×10^{-4} mol dm^{-3}, [D-fru] = 2.00×10^{-3} mol dm^{-3}, $[H^+]$ = 4.00×10^{-3} mol dm^{-3}, [Ir(III)] = 1.33×10^{-5} mol dm^{-3}, [KCl] = 1.00×10^{-5} mol dm^{-3}, [$Hg(OAc)_2$] = 3.00×10^{-4} mol dm^{-3} and CH_3COOH = 20%. Where a = Ru(III) catalysis, b = Ir(III) catalysis.

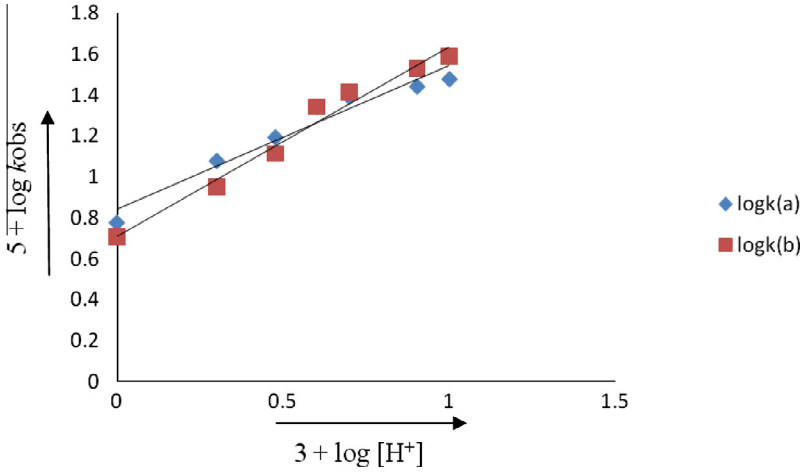

Figure 5 Plot between log k_{obs} versus log $[H^+]$ at T = 303 K. a [NBP] = 2.00×10^{-4} mol dm^{-3}, [D-fru] = 2.00×10^{-3} mol dm^{-3}, $[H^+]$ = 4.00×10^{-3} mol dm^{-3}, [Ru(III)] = 1.92×10^{-5} mol dm^{-3}, [KCl] = 1.00×10^{-5} mol dm^{-3}, [NHP] = 1.00×10^{-4} mol dm^{-3} [$Hg(OAc)_2$] = 3.00×10^{-4} mol dm^{-3} and CH_3COOH = 20%. b[NBP] = 2.00×10^{-4} mol dm^{-3}, [D-fru] = 2.00×10^{-3} mol dm^{-3}, $[H^+]$ = 4.00×10^{-3} mol dm^{-3}, [Ir(III)] = 1.33×10^{-5} mol dm^{-3}, [KCl] = 1.00×10^{-5} mol dm^{-3}, [$Hg(OAc)_2$] = 3.00×10^{-4} mol dm^{-3} and CH_3COOH = 20%. Where a = Ru(III) catalysis, b = Ir(III) catalysis.

show first-order kinetics with respect to [NBP] (Fig. 3 or Table 1) and reactions have been studied for [D-fru] (from 2.00×10^{-3} mol dm^{-3} to 10.00×10^{-3} mol dm^{-3}) at a constant concentration of all reactants at a constant temperature, this was showing zero order kinetics with respect to D-fru (Table 1). On increasing $[HClO_4]$ (from 1.00×10^{-3} mol dm^{-3} to 10.00×10^{-3} mol dm^{-3}), the value of the rate of reaction increased (Fig. 4 or Table 1). The order of reaction with respect to hydrogen ions (obtained from $HClO_4$) was determined as 0.73 from the slope of the plot between log k_{obs} and log $[H^+]$ (Fig. 5).The reaction follows positive fractional-order kinetics with respect to [Ru(III)] (from 0.96×10^{-5} mol dm^{-3} to 11.55×10^{-5} mol dm^{-3}) at a constant concentration of all reactants (Table 2). This result was further verified by the plot of k_{obs} versus [Ru(III)] (Fig. 6). The order of reaction with respect to Ru(III) was determined as 0.64 from the slope of the plot between log k_{obs} versus log[Ru(III)] (Fig. 7). The variation of $[Cl^-]$ (from 0.20×10^{-5} mol dm^{-3} to 4.00×10^{-5} mol dm^{-3}) had a negative effect on the reaction rate (Fig. 8 or Table 3). The order of reaction with respect to chloride ion was

Table 2 Effect of variation [Ru(III)] and [Ir(III)] on the rate of oxidation of D-fru at 303 K.

$[Ru(III)] \times 10^5$ mol dm^{-3}	$[Ir(III)] \times 10^5$ mol dm^{-3}	$k_{obs} \times 10^4$ s^{-1} ([a])	$k_{obs} \times 10^4$ s^{-1} ([b])
0.96	0.66	1.09	1.42
1.92	1.33	2.09	2.58
2.88	2.00	2.40	3.78
3.85	2.67	3.20	4.97
5.76	4.01	3.50	5.99
7.70	5.35	4.50	7.97
9.63	6.69	4.90	8.99
11.55	8.08	5.20	9.84

Solution conditions: (a) [NBP] = 2.00×10^{-4} mol dm^{-3}, [D-fru] = 2.00×10^{-3} mol dm^{-3}, $[H^+] = 4.00 \times 10^{-3}$ mol dm^{-3}, $[Hg(OAc)_2] = 3.00 \times 10^{-4}$ mol dm^{-3}, [Ru(III)] = 1.92×10^{-5} mol dm^{-3}, [NHP] = 1.00×10^{-4} mol dm^{-3} [KCl] = 1.00×10^{-5} mol $dm^{-3}$and CH_3COOH = 20%. (b) [NBP] = 2.00×10^{-4} mol dm^{-3}, [D-fru] = 2.00×10^{-3} mol dm^{-3}, $[H^+] = 4.00 \times 10^{-3}$ mol dm^{-3}, $[Hg(OAc)_2] = 3.00 \times 10^{-4}$ mol dm^{-3}, [Ir(III)] = 1.33×10^{-5} mol dm^{-3}, [KCl] = 1.00×10^{-5} mol dm^{-3} and CH_3COOH = 20%. Where, a = Ru(III) catalyzed, b = Ir(III) catalyzed.

[a] Ru(III)catalysis.

[b] Ir(III) catalysis.

determined as −0.62 from the slope of the plot between log k_{obs} versus log[Cl^-] (Fig. 9). While, using acetic acid (from 15% to 40%) for dielectric constant, the rate of reaction decreased with increase in the dielectric constant (D) of the medium (Fig. 10 or Table 4). The effect of the ionic strength (I) of the medium on the rate was studied using KNO_3 solution keeping the other experimental conditions constant. A negligible effect of the ionic strength of the medium and the negative effect of [NHP] were observed for Ru(III) catalyzed reaction (Table 4). Addition of phthalimide in the reaction mixture decreases the rate of oxidation in acidic media suggesting that pre-equilibrium step involves a process in which phthalimide is one of the products. Mercuric acetate used as a Br^- scavenger, did not affect the rate of reaction (Table 4). The reaction was carried out at different temperatures (298–318 K). From the linear Arrhenius plot of log k_{obs} versus $1/T$ (Fig. 11 or Table 5), the activation energy (E_a) was calculated as 55.87 $kJmol^{-1}$. Other activation parameters determined were: enthalpy of activation ($\Delta H^{\#}$ = 53.35 kJ mol^{-1}), entropy of activation ($\Delta S^{\#} = -334.45$ JK^{-1} mol^{-1}), Gibbs free energy of activation ($\Delta G^{\#}$ = 154.61 kJ mol^{-1}) and Arrhenius factor ($A = -4.65$).

3.2. Kinetics of oxidation of D-fru by NBP in the presence of Ir(III)

The values of k_{obs} at various concentrations of [NBP] (from 0.40×10^{-4} mol dm^{-3} to 2.00×10^{-4} mol dm^{-3}) clearly show first-order kinetics with respect to [NBP] (Fig. 3 or Table 1). In order to study the effect of [D-fru] on the rate of reactions a tenfold variation in [D-fru] (from 2.00×10^{-3} mol dm^{-3} to 20.00×10^{-3} mol dm^{-3}) at a constant concentration of all reactants at a fixed temperature was studied. The rate constant has been calculated at different [D-fru], this was showing zero order kinetics with respect to [D-fru] (Table 1). On increasing [$HClO_4$] concentrations (from 1.00×10^{-3} mol dm^{-3} to 10.00×10^{-3} mol dm^{-3}) the value of the rate of reaction increased (Fig. 4 or Table 1). The order of reaction with respect to hydrogen ions (obtained from $HClO_4$) was determined as 0.54 from the slope of the plot between log k_{obs} and log [H^+] (Fig. 5).The reaction follows first-order kinetics with respect to [Ir(III)] (from 0.66×10^{-5} mol dm^{-3} to 8.08×10^{-5} mol dm^{-3}) at a constant concentration of all reactants (Table 2). This result was further confirmed by the plot of

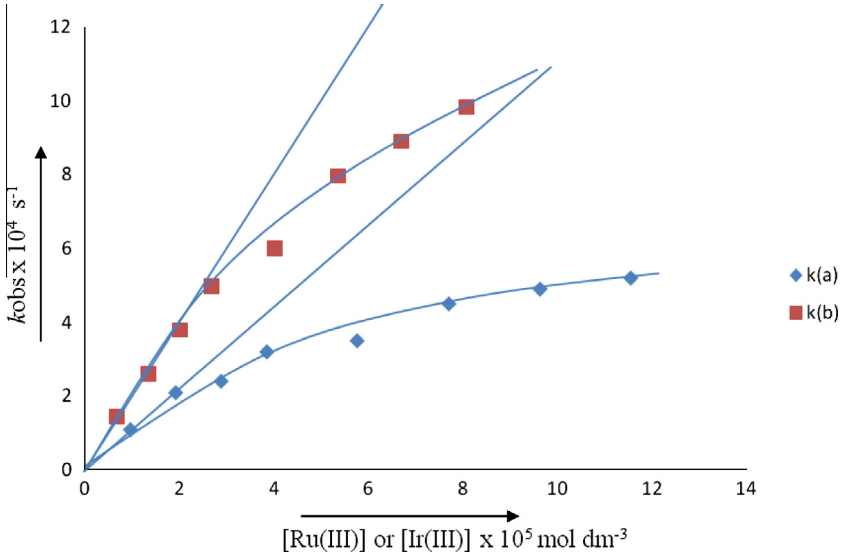

Figure 6 Plot between k_{obs} versus [Ru(III)] or [Ir(III) at T = 303 K. a [NBP] = 2.00×10^{-4} mol dm^{-3}, [D-fru] = 2.00×10^{-3} mol dm^{-3}, $[H^+] = 4.00 \times 10^{-3}$ mol dm^{-3}, [Ru(III)] = 1.92×10^{-5} mol dm^{-3}, [KCl] = 1.00×10^{-5} mol dm^{-3}, [NHP] = 1.00×10^{-4} mol dm^{-3}, $[Hg(OAc)_2] = 3.00 \times 10^{-4}$ mol dm^{-3} and CH_3COOH = 20%. b[NBP] = 2.00×10^{-4} mol dm^{-3}, [D-fru] = 2.00×10^{-3} mol dm^{-3}, $[H^+] = 4.00 \times 10^{-3}$ mol dm^{-3}, [Ir(III)] = 1.33×10^{-5} mol dm^{-3}, [KCl] = 1.00×10^{-5} mol dm^{-3}, $[Hg(OAc)_2] = 3.00 \times 10^{-4}$ mol dm^{-3} and CH_3COOH = 20%. Where a = Ru(III) catalysis, b = Ir(III) catalysis.

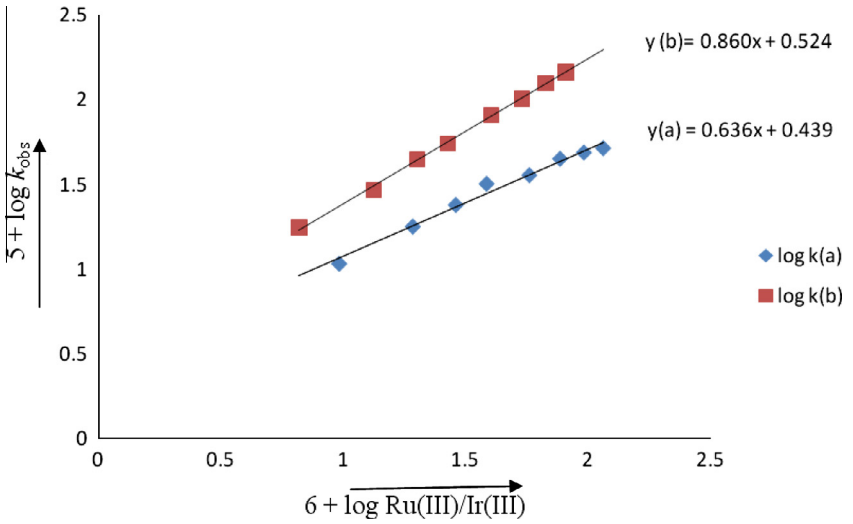

Figure 7 Plot between log k_{obs} versus log [Ru(III)] or log[Ir(III) at T = 303 K. a [NBP] = 2.00×10^{-4} mol dm^{-3}, [D-fru] = 2.00×10^{-3} mol dm^{-3}, [H^+] = 4.00×10^{-3} mol dm^{-3}, [Ru(III)] = 1.92×10^{-5} mol dm^{-3}, [KCl] = 1.00×10^{-5} mol dm^{-3}, [NHP] = 1.00×10^{-4} mol dm^{-3} [$Hg(OAc)_2$] = 3.00×10^{-4} mol dm^{-3} and CH_3COOH = 20%. b[NBP] = 2.00×10^{-4} mol dm^{-3}, [D-fru] = 2.00×10^{-3} mol dm^{-3}, [H^+] = 4.00×10^{-3} mol dm^{-3}, [Ir(III)] = 1.33×10^{-5} mol dm^{-3}, [KCl] = 1.00×10^{-5} mol dm^{-3}, [$Hg(OAc)_2$] = 3.00×10^{-4} mol dm^{-3} and CH_3COOH = 20%. Where a = Ru(III) catalysis, b = Ir(III) catalysis.

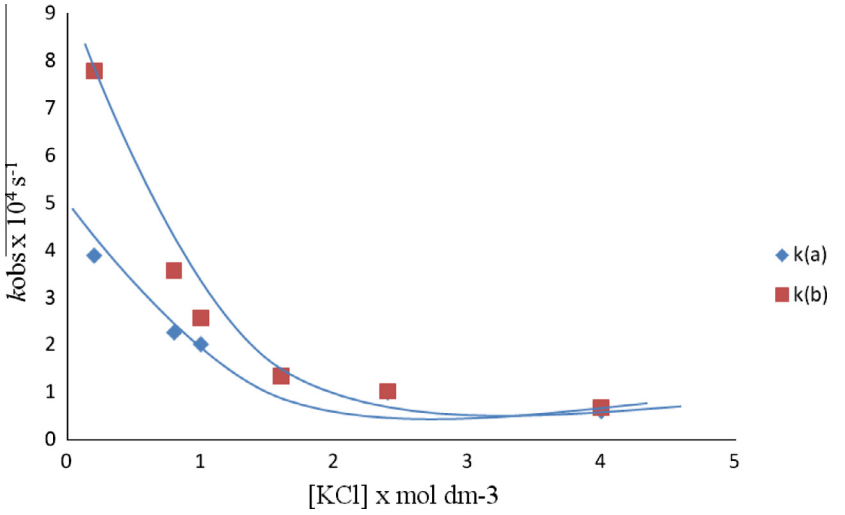

Figure 8 Plot between k_{obs} versus [KCl] at T = 303 K. a [NBP] = 2.00×10^{-4} mol dm^{-3}, [D-fru] = 2.00×10^{-3} mol dm^{-3}, [H^+] = 4.00×10^{-3} mol dm^{-3}, [Ru(III)] = 1.92×10^{-5} mol dm^{-3}, [KCl] = 1.00×10^{-5} mol dm^{-3}, [NHP] = 1.00×10^{-4} mol dm^{-3} [$Hg(OAc)_2$] = 3.00×10^{-4} mol dm^{-3} and CH_3COOH = 20%. b[NBP] = 2.00×10^{-4} mol dm^{-3}, [D-fru] = 2.00×10^{-3} mol dm^{-3}, [H^+] = 4.00×10^{-3} mol dm^{-3}, [Ir(III)] = 1.33×10^{-5} mol dm^{-3}, [KCl] = 1.00×10^{-5} mol dm^{-3}, [$Hg(OAc)_2$] = 3.00×10^{-4} mol dm^{-3} and CH_3COOH = 20%. Where a = Ru(III) catalysis, b = Ir(III) catalysis.

k_{obs} versus [Ir(III)] (Fig. 6). The order of reaction with respect to Ir(III) was determined as 0.86 from the slope of the plot between log k_{obs} versus log [Ir(III)] (Fig. 7). The variation of [Cl^-] (from 0.20×10^{-5} mol dm^{-3} to 4.00×10^{-5} mol dm^{-3}) had a negative effect on the reaction rate (Fig. 8 or Table 3). The order of reaction with respect to chloride ion was determined as −0.76 from the slope of the plot between log k_{obs} versus log[Cl^-] (Fig. 9). The variation of mercuric acetate, phthalimide and the ionic strength of the medium did not affect the reaction rate (Table 3 and 4). The dielectric constant (D) shows a slightly negative effect on the reaction rate (Fig. 10 or Table 4). The effect of temperature (from 298–318 K) on the reaction rate was determined by keeping the concentration of other constituents of the solution constant. From the linear Arrhenius plot of log k_{obs} versus $1/T$ (Fig. 11 or Table 5), the activation energy (E_a = 47.94 kJ mol^{-1}) was calculated. With the help of the energy of activation, thermodynamic parameters such as enthalpy of activation ($\Delta H^{\#}$ = 45.42 kJ mol^{-1}), entropy of activation ($\Delta S^{\#}$ = −313.00 JKmol^{-1}) and Gibbs free energy of activation ($\Delta G^{\#}$ = 140.53 kJmol^{-1}) and Arrhenius factor (A = −3.58) were calculated.

Table 3 Effect of varying [KNO_3] and [KCl] on the rate of oxidation of D-fru at 303 K.

$[KNO_3] \times 10^5$ mol dm^{-3}	$[KCl] \times 10^5$ mol dm^{-3}	$k_{obs} \times 10^4$ s^{-1} [a]	$k_{obs} \times 10^4$ s^{-1} [b]
0.20	–	2.23	2.82
0.80	–	2.14	2.78
2.40	–	2.17	2.61
4.00	–	2.13	2.70
–	0.20	3.89	7.78
–	0.80	2.26	3.56
–	1.00	2.01	2.56
–	1.60	1.36	1.33
–	2.40	0.99	1.01
–	4.00	0.59	0.66

Solution conditions: (a) [NBP] = 2.00×10^{-4} mol dm^{-3}, [D-fru] = 2.00×10^{-3} mol dm^{-3}, $[H^+] = 4.00 \times 10^{-3}$ mol dm^{-3}, $[Hg(OAc)_2] = 3.00 \times 10^{-4}$ mol dm^{-3}, [Ru(III)] = 1.92×10^{-5} mol dm^{-3}, [NHP] = 1.00×10^{-4} mol dm^{-3} [KCl] = 1.00×10^{-5} mol $dm^{-3}$and CH_3COOH = 20%. (b) [NBP] = 2.00×10^{-4} mol dm^{-3}, [D-fru] = 2.00×10^{-3} mol dm^{-3}, $[H^+] = 4.00 \times 10^{-3}$ mol dm^{-3}, $[Hg(OAc)_2] = 3.00 \times 10^{-4}$ mol dm^{-3}, [Ir(III)] = 1.33×10^{-5} mol dm^{-3}, [KCl] = 1.00×10^{-5} mol dm^{-3} and CH_3COOH = 20%. Where, a = Ru(III) catalyzed, b = Ir(III) catalyzed.

[a] Ru(III)catalysis.

[b] Ir(III) catalysis.

3.3. Test for free radicals

The intervention of free radicals was examined as follows; the reaction mixture, to which a known quantity of acryl amide had been added initially, was kept in an inert atmosphere for 24 h. When the reaction mixture was diluted with methanol, no precipitate resulted, suggesting that there is no participation of free radicals in the studied redox reaction.

3.4. Reactive species of NBP in the presence of Ru(III) and Ir(III)

It has been reported earlier by several workers (Krishnakumar et al., 2005; Khazaei and Manesh, 2005; Kirsch and Luning, 1998; Ramachandrappa et al., 1998; Kirsch et al., 1999; Day et al., 1986; Das and Indrasenan, 1986, 1987) that NBP is a good oxidizing and brominating agent because of large polarity of >N–Br bond. NBP, like other similar *N*-halo imides, may exist in various forms in acidic medium, i.e., free NBP, protonated NBP, Br^+, HOBr, $(H_2OBr)^+$, as per the following equilibria:

$$NBP + H_2O \rightleftharpoons HOBr + NHP \quad (D)$$

$$NBP + H^+ \rightleftharpoons NHP + Br^+ \quad (E)$$

$$NBP + H^+ \rightleftharpoons (NBPH)^+ \quad (F)$$

$$HOBr + H^+ \rightleftharpoons (H_2OBr)^+ \quad (G)$$

When $(H_2OBr)^+$ is taken as reactive species, the rate law obtained shows first order kinetics with respect to hydrogen ion concentrations, contrary to our observed positive fractional order in [$HClO_4$]. Therefore, the possibility of $(H_2OBr)^+$ and cationic bromine $(Br)^+$ as reactive species is ruled out. When HOBr is assumed as the reactive species, the derived law is lawfully capable to explain the negative effect of phthalimide. Hence neither of these species could be considered as the reactive species. Thus, the only choice left is NBP, which when considered as the reactive species, lead to a rate law explaining all the kinetic observations and other

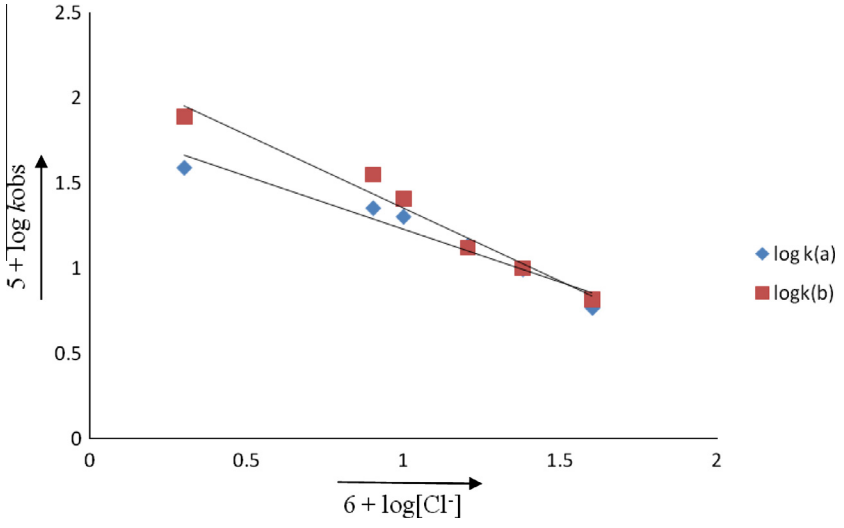

Figure 9 Plot between log k_{obs} versus log [Cl^-] at T = 303 K. a [NBP] = 2.00×10^{-4} mol dm^{-3}, [D-fru] = 2.00×10^{-3} mol dm^{-3}, $[H^+] = 4.00 \times 10^{-3}$ mol dm^{-3}, [Ru(III)] = 1.92×10^{-5} mol dm^{-3}, [KCl] = 1.00×10^{-5} mol dm^{-3}, [NHP] = 1.00×10^{-4} mol dm^{-3} $[Hg(OAc)_2] = 3.00 \times 10^{-4}$ mol dm^{-3} and CH_3COOH = 20%. b [NBP] = 2.00×10^{-4} mol dm^{-3}, [D-fru] = 2.00×10^{-3} mol dm^{-3}, $[H^+] = 4.00 \times 10^{-3}$ mol dm^{-3}, [Ir(III)] = 1.33×10^{-5} mol dm^{-3}, [KCl] = 1.00×10^{-5} mol dm^{-3}, $[Hg(OAc)_2] = 3.00 \times 10^{-4}$ mol dm^{-3} and CH_3COOH = 20%. Where a = Ru(III) catalysis, b = Ir(III) catalysis.

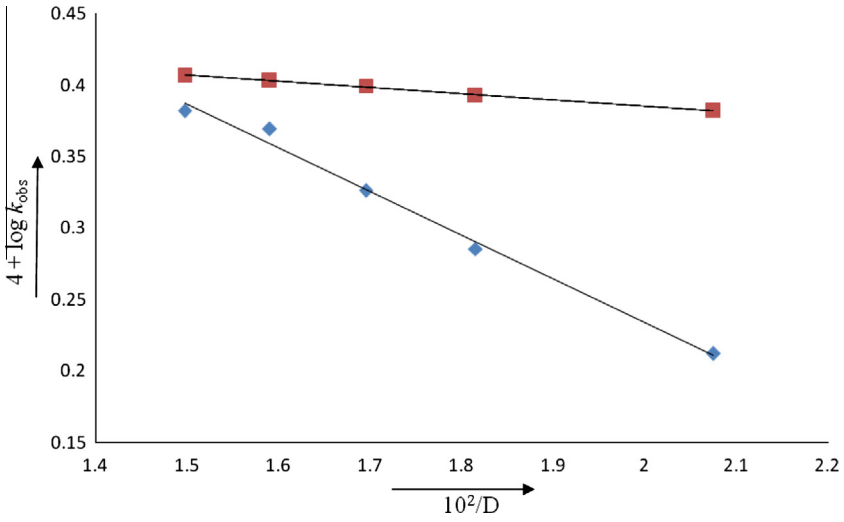

Figure 10 Plot between log k_{obs} versus 1/T. a [NBP] = 2.00×10^{-4} mol dm^{-3}, [D-fru] = 2.00×10^{-3} mol dm^{-3}, [H^+] = 4.00×10^{-3} mol dm^{-3}, [Ru(III)] = 1.92×10^{-5} mol dm^{-3}, [KCl] = 1.00×10^{-5} mol dm^{-3}, [NHP] = 1.00×10^{-4} mol dm^{-3}, [$Hg(OAc)_2$] = 3.00×10^{-4} mol dm^{-3} and CH_3COOH = 20%. b[NBP] = 2.00×10^{-4} mol dm^{-3}, [D-fru] = 2.00×10^{-3} mol dm^{-3}, [H^+] = 4.00×10^{-3} mol dm^{-3}, [Ir(III)] = 1.33×10^{-5} mol dm^{-3}, [KCl] = 1.00×10^{-5} mol dm^{-3}, [$Hg(OAc)_2$] = 3.00×10^{-4} mol dm^{-3} and CH_3COOH = 20%. Where a = Ru(III) catalysis, b = Ir(III) catalysis.

Table 4 Effect of varying [NHP], [$Hg(OAc)_2$] and dielectric constant of the medium on the rate of oxidation of D-fru at 303 K.

[NHP] × 10^4 mol dm^{-3}	Acetonitrile % by volume	[$Hg(OAc)_2$] × 10^4 mol dm^{-3}	Acetic acid % by volume	$k_{obs} \times 10^4$ s^{-1} (a)	$k_{obs} \times 10^4$ s^{-1} (b)
1.00	–	3.00	20	2.60	2.46
2.00	–	3.00	20	2.00	2.38
3.00	–	3.00	20	1.72	2.50
4.00	–	3.00	20	1.36	2.57
6.00	–	3.00	20	1.00	2.49
8.00	–	3.00	20	–	2.47
–	0	3.00	20	2.18	2.53
–	5	3.00	20	1.77	2.44
–	10	3.00	20	1.59	2.50
–	20	3.00	20	0.92	2.55
–	30	3.00	20	0.82	2.57
–	–	2.00	20	2.26	2.51
–	–	3.00	20	2.55	2.76
–	–	4.00	20	2.18	2.45
–	–	6.00	20	2.30	2.50
–	–	8.00	20	2.70	2.57
–	–	12.00	20	2.22	2.49
–	–	3.00	15	2.41	2.55
–	–	3.00	20	2.34	2.53
–	–	3.00	25	2.12	2.51
–	–	3.00	30	1.93	2.47
–	–	3.00	40	1.63	2.41

Solution conditions: (a) [NBP] = 2.00×10^{-4} mol dm^{-3}, [D-fru] = 2.00×10^{-3} mol dm^{-3}, [H^+] = 4.00×10^{-3} mol dm^{-3}, [$Hg(OAc)_2$] = 3.00×10^{-4} mol dm^{-3}, [Ru(III)] = 1.92×10^{-5} mol dm^{-3}, [NHP] = 1.00×10^{-4} mol dm^{-3}, [KCl] = 1.00×10^{-5} mol dm^{-3} and CH_3COOH = 20%. (b) [NBP] = 2.00×10^{-4} mol dm^{-3}, [D-fru] = 2.00×10^{-3} mol dm^{-3}, [H^+] = 4.00×10^{-3} mol dm^{-3}, [$Hg(OAc)_2$] = 3.00×10^{-4} mol dm^{-3}, [Ir(III)] = 1.33×10^{-5} mol dm^{-3}, [KCl] = 1.00×10^{-5} mol dm^{-3} and CH_3COOH = 20%. Where, a = Ru(III) catalyzed, b = Ir(III) catalyzed.

effects. Hence in the light of kinetic observation, NBP could be assumed to be the main reactive species for the Ru(III) catalyzed oxidation of D-fru.

In the case of Ir(III) catalyzed oxidation of D-fru, when HOBr was assumed as the reactive species, the derived rate law failed to explain the negligible effect of phthalimide. Hence

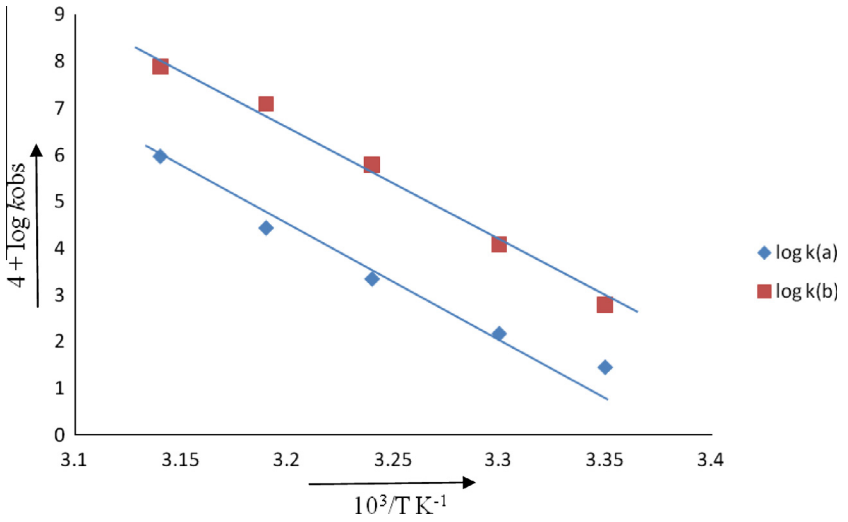

Figure 11 Plot between [NBP]/ rate versus 1/[Ru(III)] or 1/[Ir(III) at T = 303 K. a [NBP] = 2.00×10^{-4} mol dm^{-3}, [D-fru] = 2.00×10^{-3} mol dm^{-3}, $[H^+] = 4.00 \times 10^{-3}$ mol dm^{-3}, [Ru(III)] = 1.92×10^{-5} mol dm^{-3}, [KCl] = 1.00×10^{-5} mol dm^{-3}, [NHP] = 1.00×10^{-4} mol dm^{-3} $[Hg(OAc)_2] = 3.00 \times 10^{-4}$ mol dm^{-3} and CH_3COOH = 20%. b[NBP] = 2.00×10^{-4} mol dm^{-3}, [D-fru] = 2.00×10^{-3} mol dm^{-3}, $[H^+] = 4.00 \times 10^{-3}$ mol dm^{-3}, [Ir(III)] = 1.33×10^{-5} mol dm^{-3}, [KCl] = 1.00×10^{-5} mol dm^{-3}, $[Hg(OAc)_2] = 3.00 \times 10^{-4}$ mol dm^{-3} and CH_3COOH = 20%. Where a = Ru(III) catalysis, b = Ir(III) catalysis.

Table 5 Effect of temperature on the rate of oxidation of D-fru.

Temperature K	$k_{obs} \times 10^4$ s^{-1} (a)	$k_{obs} \times 10^4$ s^{-1} (b)
298	1.45	1.92
303	2.17	2.57
308	3.34	3.84
313	4.43	5.14
318	5.96	6.20

Solution conditions: (a) [NBP] = 2.00×10^{-4} mol dm^{-3}, [D-fru] = 2.00×10^{-3} mol dm^{-3}, $[H^+] = 4.00 \times 10^{-3}$ mol dm^{-3}, $[Hg(OAc)_2] = 3.00 \times 10^{-4}$ mol dm^{-3}, [Ru(III)] = 1.92×10^{-5} mol dm^{-3}, [NHP] = 1.00×10^{-4} mol dm^{-3} [KCl] = 1.00×10^{-5} mol dm^{-3} and CH_3COOH = 20%. (b) [NBP] = 2.00×10^{-4} mol dm^{-3}, [D-fru] = 2.00×10^{-3} mol dm^{-3}, $[H^+] = 4.00 \times 10^{-3}$ mol dm^{-3}, $[Hg(OAc)_2] = 3.00 \times 10^{-4}$ mol dm^{-3}, [Ir(III)] = 1.33×10^{-5} mol dm^{-3}, [KCl] = 1.00×10^{-5} mol dm^{-3} and CH_3COOH = 20%. Where, a = Ru(III) catalyzed, b = Ir(III) catalyzed.

neither of these species could be considered as the reactive species. Thus, the only choice left was NBP, which when considered as the reactive species, led to a rate law explaining all the kinetic observations and other effects. Hence in the light of kinetic observation, NBP could be assumed to be the main reactive species for the present reaction.

3.5. Reactive Species of Ru(III)

Electrochemical and spectrophotometric measurements of Ru(III) in 0.1 M KCl in the pH range of 0.4–2.0 at 25 °C suggested four major species, namely $[RuCl_4(H_2O)_2]^-$, $[RuCl_3(H_2O)_3]$, $[RuCl_2(H_2O)_4]^+$, and $[RuCl(H_2O)_5]^{2+}$ Taqui Khan et al., 1986. Except for $[RuCl_2(H_2O)_4]^+$, the stability of the species decreased with an increase in pH and a high instability at pH 2.0. The $[RuCl_2(H_2O)_4]^+$ species was however quite stable at pH 2.0, which is in equilibrium with its hydrolyzed form, $[RuCl_2(H_2O)_3OH]$ (Eq. (H)) Singh et al., 2009b,c.

$$[RuCl_2(H_2O)_4]^+ + H_2O \rightleftharpoons [RuCl_2(H_2O)_3OH] + H_3O^+ \quad (H)$$

With an increase in the concentration of the chloride ion in the experiment, the hydrolyzed form may also form $[RuCl_3(H_2O)_2OH]^-$ (C_1) through equilibrium with Cl^- ion (Eq. (I)).

$$[RuCl_2(H_2O)_3OH] + Cl^- \rightleftharpoons \underset{C_1}{[RuCl_3(H_2O)_2OH]^-} + H_2O \quad (I)$$

The observed negative effect of the chloride ion suggests that the above equilibrium is favored toward the left, therefore $[RuCl_3(H_2O)_2OH]^-$ is a true reactive species of Ru(III) chloride in the present investigation.

3.6. Reactive species of Ir(III)

A spectrophotometric study of the kinetics of the hydration of $[IrCl_6]^{3-}$ and of the addition of a Cl^- to $[Ir(H_2O)Cl_5]^{2-}$ in 1.0–2.5 M $HClO_4$ (or HCl) at 50 °C is reported (Chang and Garner, 1965). It is known that $IrCl_3$ in hydrochloric acid gives $[IrCl_6]^{3-}$ species (Cotton et al., 1999). It has also been reported that iridium (III) and iridium (I) ions are the stable species of iridium (Kravtsov and Petrova, 1964). Further, the equation of $[IrCl_6]^{3-}$ gives $[IrCl_5H_2O]^{2-}$, $[IrCl_4(H_2O)_2]^-$ and $[IrCl_3(H_2O)_3]$ species Poulsen and Garner, 1962; Domingos et al., 1969; Frost and Pearson, 1961. This equilibrium may be shown by the general equation.

$$IrCl_6^{3-} + n - H_2O \rightleftharpoons [IrCl_6 - (H_2O)n]^{3-n} + Cl^- \quad (J)$$

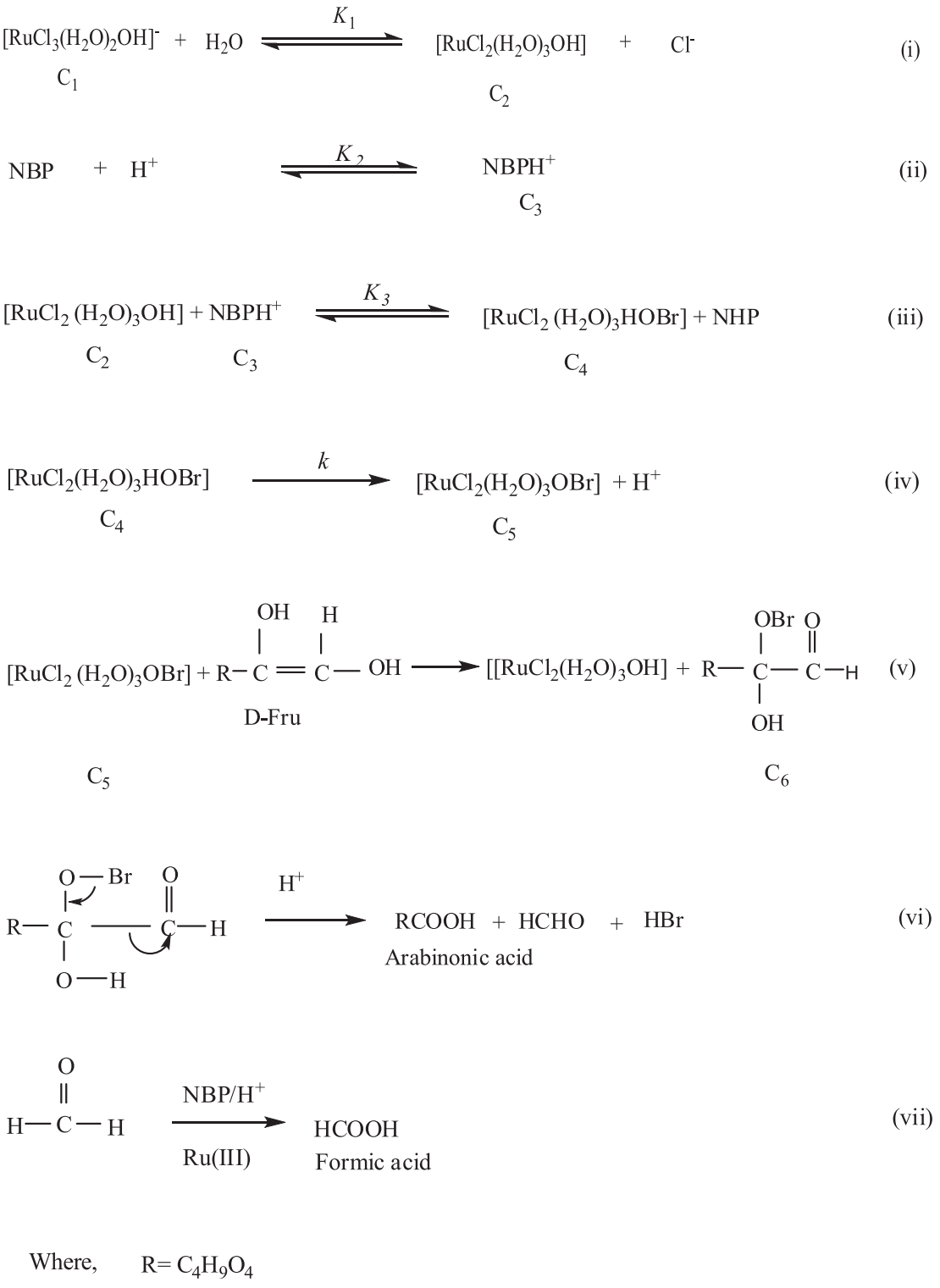

Scheme 1 Reaction path for the oxidation of D-fru by NBP in the presence of Ru(III).

Positive effect of chloride ions on the reaction rate in the present study indicates that $[IrCl_5(H_2O)]^{2-}$ cannot be considered as the reactive species. Therefore, considering our experimental results, $[IrCl_6]^{3-}$ can be considered to be the reactive species of iridium (III) chloride in the present study.

3.7. Reaction mechanism and rate law in the presence of Ru(III)

Considering the reactive species of Ru(III) and NBP and with the help of the above experimental findings, the probable reaction mechanism is proposed. In reaction Scheme 1, the

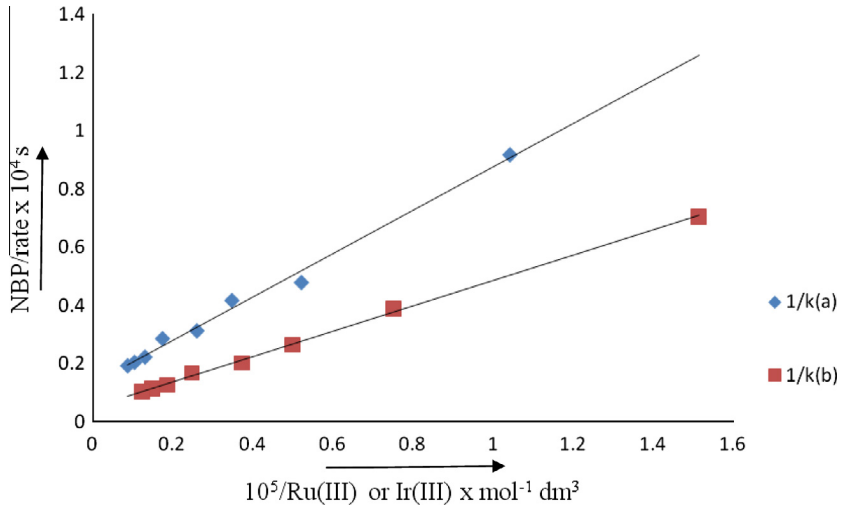

Figure 12 Plot between [NBP]/ rate versus $1/[H^+]$ at T = 303 K. a [NBP] = 2.00×10^{-4} mol dm^{-3}, [D-fru] = 2.00×10^{-3} mol dm^{-3}, $[H^+] = 4.00 \times 10^{-3}$ mol dm^{-3}, [Ru(III)] = 1.92×10^{-5} mol dm^{-3}, [KCl] = 1.00×10^{-5} mol dm^{-3}, [NHP] = 1.00×10^{-4} mol dm^{-3} [$Hg(OAc)_2$] = 3.00×10^{-4} mol dm^{-3} and CH_3COOH = 20%. b[NBP] = 2.00×10^{-4} mol dm^{-3}, [D-fru] = 2.00×10^{-3} mol dm^{-3}, $[H^+] = 4.00 \times 10^{-3}$ mol dm^{-3}, [Ir(III)] = 1.33×10^{-5} mol dm^{-3}, [KCl] = 1.00×10^{-5} mol dm^{-3}, [$Hg(OAc)_2$] = 3.00×10^{-4} mol dm^{-3} and CH_3COOH = 20%. Where a = Ru(III) catalysis, b = Ir(III) catalysis.

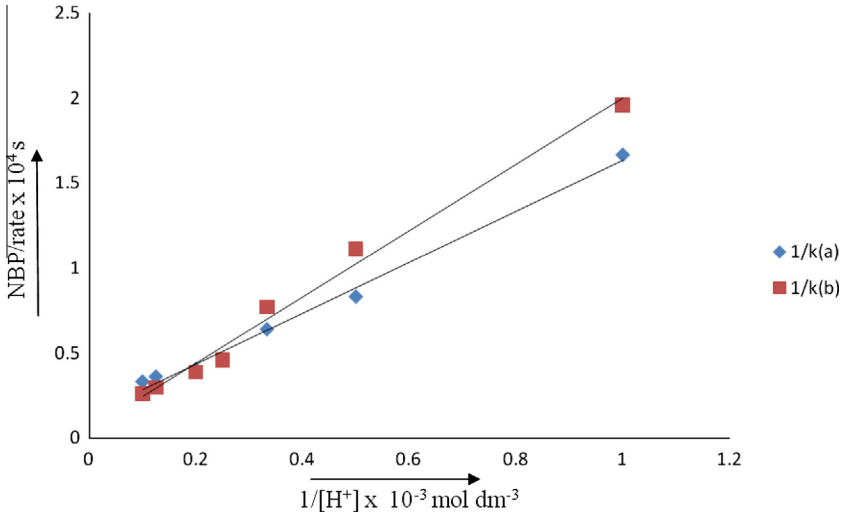

Figure 13 Sample individual [NHP] plots for $1/k_{obs}$ at 303 a [NBP] = 2.00×10^{-4} mol dm^{-3}, [D-fru] = 2.00×10^{-3} mol dm^{-3}, $[H^+] = 4.00 \times 10^{-3}$ mol dm^{-3}, [Ru(III)] = 1.92×10^{-5} mol dm^{-3}, [KCl] = 1.00×10^{-5} mol dm^{-3}, [NHP] = 1.00×10^{-4} mol dm^{-3} [$Hg(OAc)_2$] = 3.00×10^{-4} mol dm^{-3} and CH_3COOH = 20%. Where a = Ru(III) catalysis.

reaction between NBP and D-fru in the acidic medium in the presence of Ru(III) has a 1:2 stoichiometry of oxidant to reductant with first order dependence on [NBP]. reaction Scheme 1 also suggested an apparent order, less than unit order, in [Ru(III)] and $[H^+]$ in the rate of reaction. In this scheme, the species C_2 is formed from the reaction of C_1 on hydrolysis with the liberation of Cl^- and species C_1 and C_2 are in equilibrium having a constant K_1 [Eq. (1)]. Protonated NBP i.e. C_3 formed in step II having a constant K_2 [Eq. (2)]. The species C_2 and C_3 react to give brominated species, [$RuCl_2(H_2O)_3HOBr$] (C_4), and phthalimide (NHP) [Eq. (3)]. The species C_4 gives C_5 and proton [Eq. (4)] in the rate determining step. The species C_5 brominates the D-fru molecule to form C_6 [Eq. (5)]. The species C_6 forms RCOOH and HCOOH as major products of the reaction by fast steps [Eq. (6) and (7)]. Overall, reaction Scheme 1 gives a consumption of two molecules of NBP per molecule of D-fru, consistent with the observed stoichiometry.

On the basis of reaction Scheme 1, the rate in terms of decrease in the concentration of NBP can be expressed as:

$$\text{Rate} = 2k[C_4] \tag{1}$$

On the basis of steps (1) to (6), Eqs. (2)–(9) can be obtained in the following forms, respectively:

$$[C_2] = \frac{K_1[C_1]}{[Cl^-]} \tag{2}$$

$$[C_3] = K_2[NBP][H^+] \quad (3)$$

$$[C_4] = \frac{K_2[C_3][C_2]}{[NHP]} \quad (4)$$

Putting the value of $[C_2]$ and $[C_3]$ in above equation, we have

$$= \frac{K_1K_2K_3[NBP][H^+][C_1]}{[Cl^-][NHP]} \quad (5)$$

Substitution of Eq. (5) into Eq. (1) gives

$$\text{Rate} = \frac{2kK_1K_2K_3[NBP][H^+][C_1]}{[Cl^-][NHP]} \quad (6)$$

At any time of the reaction, the total concentration of NBP, i.e. $[NBP]_T$ can be shown as

$$[NBP]_T = [NBP] + C_3 + C_4 \quad (7)$$

On substituting the value of $[C_3]$ & $[C_4]$ in Eq. (7) we get Eq. (8)

$$= [NBP] + K_2[NBP][H^+] + \frac{K_1K_2K_3[NBP][H^+][C_1]}{[Cl^-][NHP]} \quad (8)$$

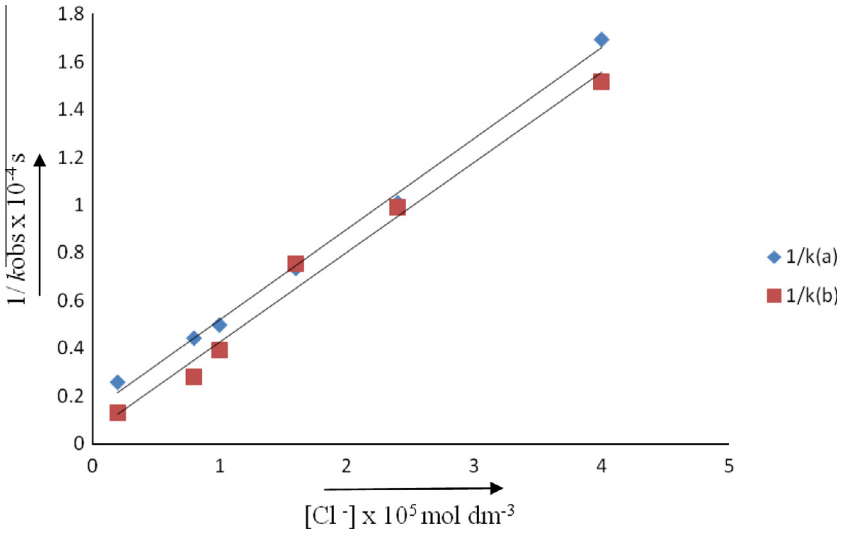

Figure 14 Plot between $1/k_{obs}$ versus $[Cl^-]$ at T = 303 K. a $[NBP] = 2.00 \times 10^{-4}$ mol dm^{-3}, [D-fru] = 2.00×10^{-3} mol dm^{-3}, $[H^+] = 4.00 \times 10^{-3}$ mol dm^{-3}, $[Ru(III)] = 1.92 \times 10^{-5}$ mol dm^{-3}, $[KCl] = 1.00 \times 10^{-5}$ mol dm^{-3}, $[NHP] = 1.00 \times 10^{-4}$ mol dm^{-3} $[Hg(OAc)_2] = 3.00 \times 10^{-4}$ mol dm^{-3} and CH_3COOH = 20%. b$[NBP] = 2.00 \times 10^{-4}$ mol dm^{-3}, [D-fru] = 2.00×10^{-3} mol dm^{-3}, $[H^+] = 4.00 \times 10^{-3}$ mol dm^{-3}, $[Ir(III)] = 1.33 \times 10^{-5}$ mol dm^{-3}, $[KCl] = 1.00 \times 10^{-5}$ mol dm^{-3},$[Hg(OAc)_2] = 3.00 \times 10^{-4}$ mol dm^{-3} and CH_3COOH = 20%. Where a = Ru(III) catalysis, b = Ir(III) catalysis.

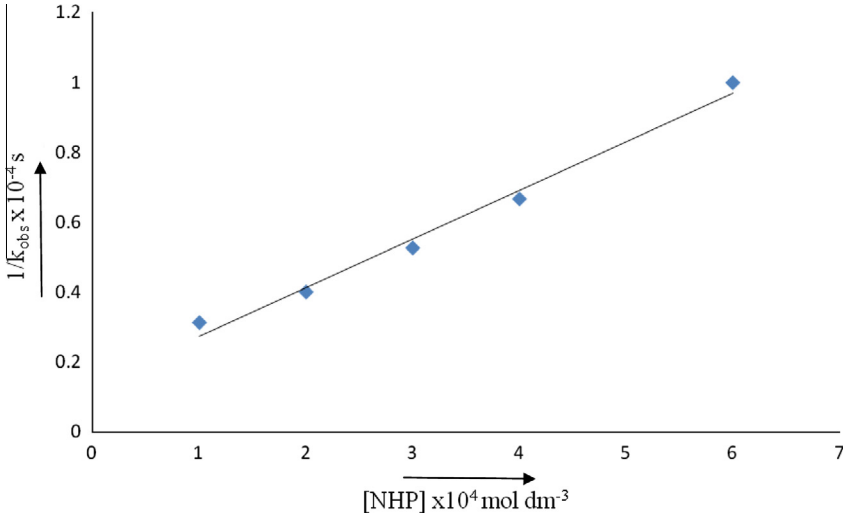

Figure 15 Plot between log k_{obs} versus 1/D.0 a $[NBP] = 2.00 \times 10^{-4}$ mol dm^{-3}, [D-fru] = 2.00×10^{-3} mol dm^{-3}, $[H^+] = 4.00 \times 10^{-3}$ mol dm^{-3}, $[Ru(III)] = 1.92 \times 10^{-5}$ mol dm^{-3}, $[KCl] = 1.00 \times 10^{-5}$ mol dm^{-3}, $[NHP] = 1.00 \times 10^{-4}$ mol dm^{-3} $[Hg(OAc)_2] = 3.00 \times 10^{-4}$ mol dm^{-3} and CH_3COOH = 20%. b $[NBP] = 2.00 \times 10^{-4}$ mol dm^{-3}, [D-fru] = 2.00×10^{-3} mol dm^{-3}, $[H^+] = 4.00 \times 10^{-3}$ mol dm^{-3}, $[Ir(III)] = 1.33 \times 10^{-5}$ mol dm^{-3}, 0 $[KCl] = 1.00 \times 10^{-5}$ mol dm^{-3}, $[Hg(OAc)_2] = 3.00 \times 10^{-4}$ mol dm^{-3} and CH_3COOH = 20%. Where a = Ru(III) catalysis, b = Ir(III) catalysis.

$$[\mathrm{NBP}] = \frac{[\mathrm{NBP}]_T[\mathrm{Cl}^-][\mathrm{NHP}]}{K_2[\mathrm{Cl}^-][\mathrm{NHP}][\mathrm{H}^+] + K_1K_2K_3[\mathrm{H}^+][\mathrm{C}_1]} \quad (9)$$

But

$$[\mathrm{C}_1] = [\mathrm{Ru(III)}]$$

$$\mathrm{Rate} = \frac{2kK_1K_2K_3[\mathrm{NBP}]_T[\mathrm{Ru(III)}][\mathrm{H}^+]}{[\mathrm{Cl}^-][\mathrm{NHP}] + K_2[\mathrm{Cl}^-][\mathrm{NHP}] + K_1K_2K_3[\mathrm{H}^+][\mathrm{Ru(III)}]} \quad (10)$$

or

$$\mathrm{Rate} = \frac{2kK_1K_2K_3[\mathrm{NBP}]_T[\mathrm{Ru(III)}][\mathrm{H}^+]}{[\mathrm{Cl}^-][\mathrm{NHP}](1 + K_2[\mathrm{H}^+]) + K_1K_2K_3[\mathrm{H}^+][\mathrm{Ru(III)}]} \quad (11)$$

Since $[\mathrm{H}^+]$ is on the order of 10^{-3}, the inequality $K_2[\mathrm{H}^+]$ 1, can be taken as a valid one. With this inequality, Eq. (11) is converted to Eq. (12).

$$\mathrm{Rate} = \frac{2kK_1K_2K_3[\mathrm{NBP}]_T[\mathrm{Ru(III)}][\mathrm{H}^+]}{[\mathrm{Cl}^-][\mathrm{NHP}] + K_1K_2K_3[\mathrm{H}^+][\mathrm{Ru(III)}]} \quad (12)$$

The rate expression obtained in Eq. (11) can be re-written as

$$\frac{[\mathrm{NBP}]_T}{\mathrm{Rate}} = \frac{[\mathrm{Cl}^-][\mathrm{NHP}]}{2kK_1K_2K_3[\mathrm{Ru(III)}][\mathrm{H}^+]} + \frac{1}{2k} \quad (13)$$

Eq. (13), indicates that if the graph is plotted between $[\mathrm{NBP}]_T$/rate and 1/[Ru(III)], 1/$[\mathrm{H}^+]$, $[\mathrm{Cl}^-]$ and [NHP], a straight line with a positive intercept on the y-axis will be obtained. Straight

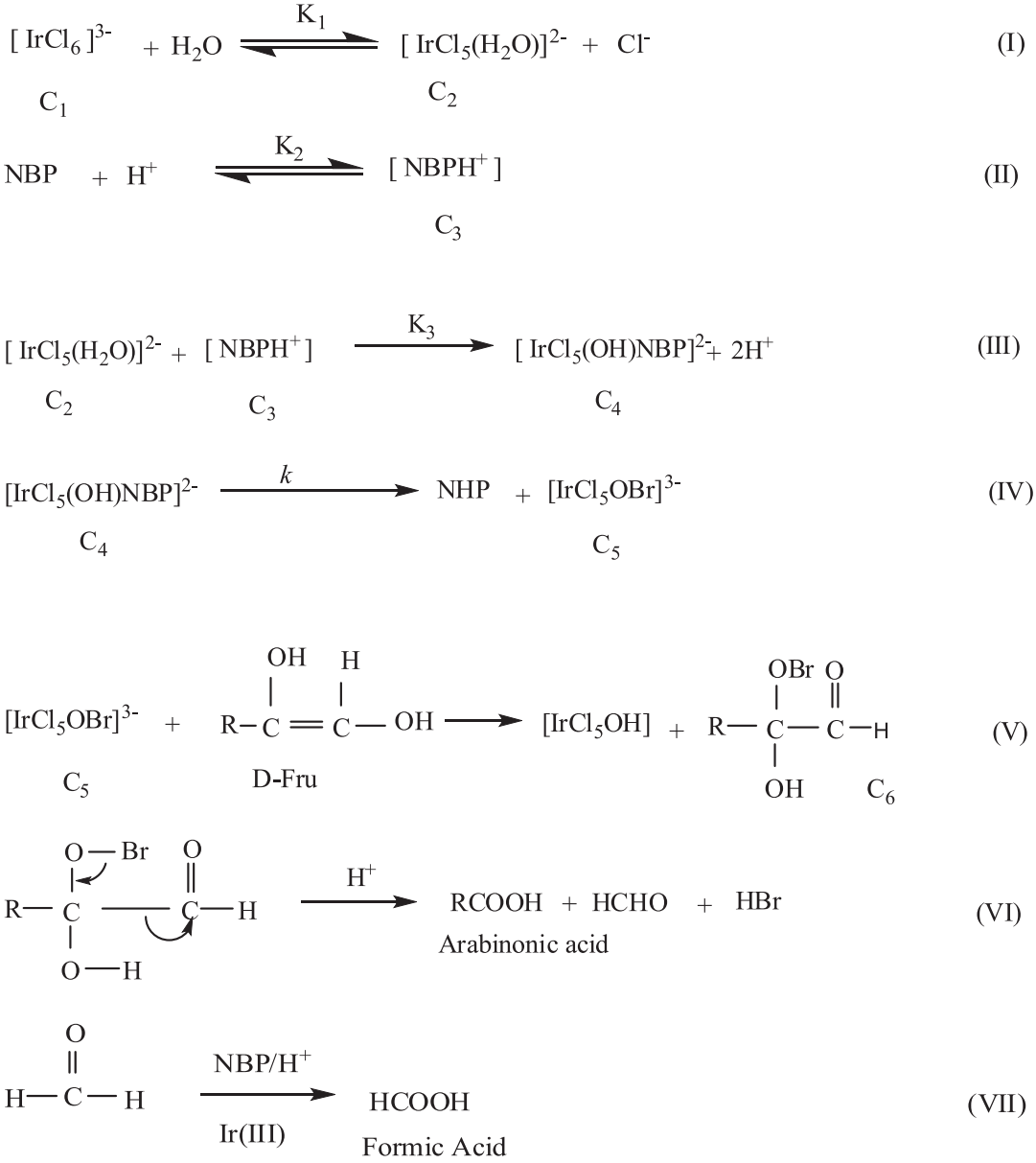

Where, R= $C_4H_9O_4$

Scheme 2 Reaction path for the oxidation of D-fru by NBP in the presence of Ir(III).

line with positive intercepts on the y-axis obtained by the plots of $[NBP]_T$/rate versus 1/[Ru(III)], 1/$[H^+]$, $[Cl^-]$ and [NHP] (Fig. 12–15) on the one hand proves the validity of the rate law (12). The value of k, and $K_1K_2K_3$ calculated from the slope and intercept of the plot were 3.62×10^{-4}, 4.49×10^{-3} mol dm^{-3}, respectively.

3.8. Reaction mechanism and rate law in the presence of Ir(III)

On the basis of observed kinetic results by taking $[IrCl_6]^{3-}$ as the most active species of Ir(III) and NBP itself as reactive species Reaction Scheme 2 is proposed on the basis of all the steps for the oxidation of D-fru considering the fact that 1 mol of D-fru is oxidized by 2 mol of NBP.

In this scheme, the species C_2 is formed from the reaction of C_1 with the water molecule and species C_1 and C_2 are in equilibrium having a constant K_1 (Eq. (1)). In the second step, NBP reacts with H^+ to form protonated NBP i.e. C_3 in equilibrium with a constant K_2 (Eq. (2)). The species C_2 reacts with C_3 to give species C_4 having an equilibrium constant K_3 with the liberation of proton (Eq. (3)). The species C_4 slowly decomposes to give brominated species, $[IrCl_5(OBr)]^{3-}$ (C_5) and phthalimide (NHP) (Eq. (4)). The species C_5 brominates the D-fru molecule to form C_5 (intermediate species). The intermediate species C_5 brominates the D-fru molecule to form C_6 (Eq. (5)). The species C_6 forms RCOOH and HCOOH as major products of the reaction by fast steps (Eq. (6) and (7)).

On the basis of the reaction scheme 2, the rate in terms of decrease in the concentration of NBP can be expressed as:

$$\text{Rate} = 2k[C_4] \tag{14}$$

On the basis of steps (I) to (VII), Eqs. (15)–(18) can be obtained in the following forms, respectively:

K_2

$$[C_2] = \frac{K_1[C_1]}{[Cl^-]} \tag{15}$$

$$[C_3] = K_2[NBP][H^+] \tag{16}$$

$$[C_4] = K_3[C_2][C_3] \tag{17}$$

With the help Eq. (15) and (16) we can write Eq. (17) as

$$[C_4] = \frac{K_1K_2K_3[C_1][NBP][H^+]}{[Cl^-]} \tag{18}$$

At any moment of the reaction, the total concentration of [NBP], i.e. $[NBP]_T$ can be represented as

$$[NBP]_T = [NBP] + [C_3] + [C_4] \tag{19}$$

On substituting the value of $[C_3]$ and $[C_4]$, we get Eq. (20)

$$[NBP]_T = [NBP] + K_2[NBP][H^+] + \frac{K_1K_2K_3[C_1][NBP][H^+]}{[Cl^-]} \tag{20}$$

With the help of Eqs. (19) and (14) we can write Eq. (20) as

$$\text{Rate} = \frac{2kK_1K_2K_3[C_1][H^+][NBP]_T}{[Cl^-] + K_2[H^+][Cl^-] + K_1K_2K_3[C_1][H^+]} \tag{21}$$

Eq. (21) is the rate law on the basis of which observed kinetic orders with respect to each reactant of the reaction can very easily be explained. Eq. (21) can be written as:

$$\frac{\text{Rate}}{[NBP]_T} = \frac{2kK_1K_2K_3[C_1][H^+]}{[Cl^-] + K_2[H^+][Cl^-] + K_1K_2K_3[C_1][H^+]} \tag{22}$$

The rate expression obtained in Eq. (22) can be re-written as

$$\frac{[NBP]_T}{\text{Rate}} = \frac{1}{k_1} = \frac{[Cl^-]}{2kK_1K_2K_3[C_1][H^+]} + \frac{[C_1]}{2kK_1K_3[C_1]} + \frac{1}{2k} \tag{23}$$

According to Eq. (23), if a graph is plotted between [NBP]/rate versus 1/ [Ir(III)], 1/$[H^+]$ and $[Cl^-]$, a straight line having an intercept on the y-axis will be obtained (Fig. 12–14). This proves the validity of the rate law (21) and the proposed Reaction Scheme 2. From the slope and intercept of the straight lines, the values of k, $K_1K_2K_3$ and K_1K_3 have been calculated and are found to be 1.03×10^{-3}, 1.85×10^{1} and 1.64×10^{-1} respectively.

3.9. Activation parameters

Activation parameters are believed to provide useful information regarding the environment in which chemical reactions take place. The effects of changing the solvent composition on the rate of reaction have been discussed in detail in the well known publications by Frost and Pearson (Frost and Pearson, 1961). For the limiting case of zero angle approach between two dipoles or an ion–dipole system, Emis (Emis, 1966) has shown that a plot of log k versus $1/D$ gives a straight line, with a negative slope for a reaction between a negative ion and a dipole or between two dipoles, while a positive slope results for a

Table 6 (a) Consumption of NBP in the [Ru(III)] catalyzed oxidation of D- Fru with NBP at 303 K (b) Consumption of NBP in the [Ir(III)] catalyzed oxidation of D-fru with NBP at 303 K.

[D-fru] × 10^4 mol dm^{-3}	[NBP] × 10^4 mol dm^{-3m} Initial	[NBP] × 10^4 mol dm^{-3} Final	[NBP] × 10^4 mol dm^{-3} Consumed	[NBP]: [D-fru]
a				
2.00	20.00	16.00	4.06	1:2.03
4.00	40.00	31.87	8.16	1:2.04
6.00	60.00	47.79	12.30	1:2.05
b				
2.00	20.00	15.86	4.08	1:2.06
4.00	40.00	31.94	8.20	1:2.05
6.00	60.00	48.89	12.22	1:2.03

positive ion–dipole interaction. The former concept agrees with the present investigation. The reactions were studied at five different temperatures (298 K–318 K) to calculate activation parameter. From the plot of log k_{obs} versus $1/T$ (Arrhenius plot, Fig. 10), the activation energy (E_a) was evaluated. The proposed mechanism is also supported by the moderate values obtained for energy of activation and other thermodynamic parameters. The positive values of free energy of activation and of the enthalpy of activation suggests that the transition state is highly solvated, while the high negative entropy of activation indicates that transition state is highly associated. The order of frequency factor (A) and values of free energy of activation ($\Delta G^{\#}$) for the redox system also supports a reaction scheme proposed for the oxidation of D-fru by NBP in the presence of Ru(III) chloride under acidic conditions.

Table 7 Comparison of observed rates in the variation of [Ru(III)], [H^+] & [KCl] with predicted rates for the oxidation of D-fru with NBP at 303 K.

[Ru(III)] × 10^5 (mol dm^{-3})	[H^+] × 10^3 (mol dm^{-3})	[KCl] × 10^5 (mol dm^{-3})	$k_1 \times 10^4$ (s^{-1}) (Observed)	$k_1 \times 10^4$ (s^{-1}) (Calculated)	$k_1 \times 10^4$ (s^{-1}) (Predicted)
0.96	4.00	1.00	1.09	1.06	1.38
1.92	4.00	1.00	2.09	1.85	2.10
3.85	4.00	1.00	3.20	2.95	2.69
7.70	4.00	1.00	4.50	4.20	4.11
9.63	4.00	1.00	4.90	4.57	4.90
11.55	4.00	1.00	5.20	4.88	5.61
1.92	1.00	1.00	0.60	0.57	0.75
1.92	2.00	1.00	1.20	0.72	1.25
1.92	4.00	1.00	2.19	1.86	1.69
1.92	5.00	1.00	2.46	2.18	2.10
1.92	8.00	1.00	2.76	2.95	2.49
1.92	10.00	1.00	3.00	3.35	3.54
1.92	4.00	0.20	4.20	4.57	3.03
1.92	4.00	0.80	3.00	2.17	2.21
1.92	4.00	1.00	2.10	1.86	2.10
1.92	4.00	1.60	0.90	1.28	1.89
1.92	4.00	2.40	0.43	0.90	1.53

k_{obs} = Calculated with the help of graph between log (a-x) versus T.
k_{cal} = Calculated on the basis of rate law.
k_{pre} = Calculated with the help of multiple regression analysis.

Table 8 Comparison of observed rates in the variation of [Ir(III)], [H^+] & [KCl] with predicted rates for the oxidation of D-fru with NBP at 303 K.

[Ir(III)] × 10^5 (mol dm^{-3})	[H^+] × 10^3 (mol dm^{-3})	[KCl] × 10^5 (mol dm^{-3})	$k_1 \times 10^4$ (s^{-1}) (Observed)	$k_1 \times 10^4$ (s^{-1}) (Calculated)	$k_1 \times 10^4$ (s^{-1}) (Predicted)
0.66	4.00	1.00	1.42	1.24	1.43
1.33	4.00	1.00	2.58	2.16	2.16
2.67	4.00	1.00	4.97	4.02	3.26
4.01	4.00	1.00	5.99	5.60	5.14
6.69	4.00	1.00	8.99	8.20	8.26
8.08	4.00	1.00	9.84	9.30	9.53
1.33	1.00	1.00	0.51	0.82	1.36
1.33	2.00	1.00	0.90	1.40	1.78
1.33	3.00	1.00	2.22	1.84	2.16
1.33	4.00	1.00	2.60	2.16	2.51
1.33	8.00	1.00	3.40	3.00	3.44
1.33	10.00	1.00	3.90	3.26	4.00
1.33	4.00	0.20	7.78	8.12	7.74
1.33	4.00	0.80	3.56	2.66	2.33
1.33	4.00	1.00	2.56	2.16	2.16
1.33	4.00	1.60	1.33	1.40	1.84
1.33	4.00	2.40	1.01	0.94	1.60
1.33	4.00	4.00	0.66	0.56	1.35

k_{obs} = Calculated with the help of graph between log (a-x) vs T.
k_{cal} = Calculated on the basis of rate law.
k_{pre} = Calculated with the help of multiple regression analysis.

3.10. Effect of the dielectric constant and calculation of the size of an activated complex (d_{AB}) in the oxidation of D-fru

In order to find out the effect of the dielectric constant of the medium on the reaction rate, the reaction has been studied with different dielectric constants (D) of the medium at a constant concentration of all other reactants and at a constant temperature. It is clear from the Table 4 that k (rate constant) values decreased with the decreased rate constant on the dielectric constant of the medium as given by the following equation:

$$\log k = \log K_0 = -\frac{Z_A Z_B e^2 N}{2.303(4\pi\varepsilon_0)d_{AB}\mathrm{DRT}} \quad (24)$$

where k_0 is the rate constant in a medium of infinite dielectric constant, Z_A and Z_B are the charges of reacting ions, d_{AB} refers to the size of the activated complex, and T is absolute temperature and D is the dielectric constant of the medium. This equation suggests that if a plot is made between log k_{obs} vs $1/D$, a straight line can be attained with slopes of -0.306 in Ru(III) catalyzed and -0.043 in Ir(III) catalyzed oxidation of D-fru. A negative dielectric effect supports the proposed mechanism. The effects of changing the solvent compositions on the rate of reaction have been discussed in detail (Moelwyn-Hughes, 1974, 1961; Laidler and Eyring, 1940; Laidler and Landskroener, 1957; Laidler, 1963; Benson, 1960; Frost and Pearson, 1961; Entelis and Tiger, 1976). For the limiting case of the zero angle approach between two dipoles or an ion–dipole system, it has been shown that a negative slope of a linear line in the plot of log k versus $1/D$ is a general result for a reaction between a negative ion and a dipole or between two dipoles. A positive slope relates to a positive ion–dipole interaction (Morris et al., 1948). The former concept agrees with the observations in the present study. The values of d_{AB} were evaluated using slopes as 7.81 Å and 0.55 Å in Ru(III) and Ir(III) catalyzed, respectively(Fig. 15).

3.11. Multiple regression analysis

In order to find out the relationship between dependent variable log $k_{(\text{calculated + observed + predicted})}$ and three independent variables, log [Ru(III)], log [H^+] and log [Cl^-] in Ru(III) catalyzed (Table 7) and log [Ir(III)], log [H^+] and log [Cl^-] in Ir (III) catalyzed (Table 8) and to arrive at a conclusion whether the proposed mechanism is well in accordance with our experimental kinetic data or not, we have taken multiple regression analyses using the computer package 'STATGRAPHICS'. For Ru(III) catalyzed and Ir(III) catalyzed oxidation, the output shows the results of multiple regression relationship between log $k_{(\text{calculated + observed + predicted})}$ and independent variables. With the help of a multivariate regression analysis a relationship between the observed pseudo first order rate constant (k_{obs}) and concentrations of all the reactants of the reaction of the reaction was found to be:

$$k_{obs} = k[\mathrm{Ru(III)}]^{0.61}[\mathrm{H^+}]^{0.75}[\mathrm{Cl^-}]^{-0.22} \quad (25)$$

$$k_{obs} = k[\mathrm{Ir(III)}]^{0.94}[\mathrm{H^+}]^{-0.56}[\mathrm{Cl^-}]^{0.52}[\mathrm{NHP}]^{-0.20} \quad (26)$$

where $k = 7.21 \times 10^{-1}$ and 6.75×10^{-1} for Ru(III) and Ir(III) catalyzed reaction respectively.

In both the cases, as the p-value in the ANOVA is less than 0.01, there is a statistically significant relationship between the variables at the 99% confidence level. This supports the validity of the rate laws given in Eqs. (12) and (21) for the Ru(III) and Ir(III) catalyzed oxidation, respectively. The proposed reactions in Reaction Schemes 1 and 2 are also valid because these equations were used to calculate the rates based on the multiple regression analysis (Eqs. (25) and (26)). The similarity among the three rates, i.e., the observed (experimentally), calculated (from rate law), and predicted (from regression analysis) results, clearly support the validity of the rate laws expressed in Eqs. (12) and (21), and the proposed reaction mechanisms.

4. Comparative study

Efforts were also made to compare the findings in this work with results already reported (Singh et al., 2004) for the mechanism of Ir(III)-catalyzed and Hg(II)-co-catalyzed oxidation of reducing sugars by N-bromoacetamide in acidic medium and for first and novel oxidation of D-fructose by potassium iodate using $[IrCl_3(H_2O)_2OH]^-$ complex as a homogeneous catalyst in alkaline medium (Singh et al., 2008). The observed negligible effect of Hg(II) ion in each case, clearly distinguishes the present investigation from the other one (Singh et al., 2004) where a positive effect of Hg(II) ion was observed. On the basis of nil effect in [Hg(II)], it is concluded that the role of Hg(II) is limited only up to its function as a Br^- ion scavenger in the present studies. The present study differs entirely from another study (Singh et al., 2004) with respect to [H^+]. The observed positive order in both the catalysts clearly demarcates the present investigation from the other one where the negative order was found. The present work shows similarity with Ir(III)-catalyzed and Hg(II)-co-catalyzed oxidation of reducing sugars by N-bromoacetamide in acidic medium and first and novel oxidation of D-fructose by potassium iodate using $[IrCl_3(H_2O)_2OH]^-$ complex as a homogeneous catalyst in alkaline medium being zero order with respect to [D-fru]. The observed zero effect of D-fru concentration can be viewed in a different way by negating the possibilities of the formation of an active complex between the reactive species of Ru(III) or Ir(III) and the D-fru. The reported (Singh et al., 2004) negative effect in [NHA] for Ir(III)-catalyzed and Hg(II)-co-catalyzed oxidation seems to be similar to the present study as far as the negative effect of [NHP] with respect to Ru(III) is concerned, but dissimilar as far as the nil effect with respect to Ir (III) is concerned. In the present study, the rate of reaction decreased with increasing concentration of chloride ion similar to the earlier reported (Singh et al., 2004) work but when the results of the present study were compared to the chloride ion in the oxidation of D-fructose by potassium iodate (Singh et al., 2008), nil effect on the rate of reaction was found. The change in the ionic strength (μ) has no effect on oxidation velocity in all studies. On the basis of the observed kinetic data, it can be concluded that $[RuCl_3(H_2O)_2OH]$ is the reactive species of Ru(III) chloride and $[IrCl_6]^{3-}$ is the reactive species of Ir(III) chloride in the present study of the oxidation of D-fru in acidic medium, whereas in the reported (Singh et al., 2004) work the reactive species of Ir(III) chloride was found to be $[IrCl_5(H_2O)]^{2-}$ and $[IrCl_3H_2O)_2OH]^-$ is the reactive species of Ir(III) in the oxidation of fructose in alkaline medium (Singh et al., 2008).

5. Conclusions

Oxidation of D-fru by NBP in perchloric acid medium was found to be very sluggish, but oxidation became facile in the presence of micro-quantity of Ru (III) chloride catalyst or Ir (III) chloride catalyst. $[RuCl_3(H_2O)_2OH]$ and $[IrCl_6]^{3-}$ have been assumed as the reactive species of Ru(III) chloride and Ir(III) chloride in the oxidation of D-fru in acidic medium, respectively. The rate of oxidation of D-fru is unaffected by the ionic strength of the medium in both catalysts. The observed zero effect of D-fru concentration can be viewed in a different way by negating the possibility of the formation of an active complex between the reactive species of Ru(III) or Ir(III) and D-fru. The negative entropy of activation in both cases showss that the activated complex would be more extensively solvated than the reactive species. The observed results were explained by plausible mechanisms and the related rate laws were deduced. It can be concluded that both Ru(III) and Ir(III) act as an efficient catalyst for the oxidation of D-fru by NBP in acidic medium. The values of energy of activation (Ea) indicate that the rate of Ir(III) catalyzed oxidation reaction is faster than Ru(III) catalyzed reaction.

Acknowledgement

We wish to thank reviewers for the critical and useful comments that refined the manuscript a lot.

References

Benson, S.W., 1960. The Foundations of Chemical Kinetics. McGraw-Hill, New York.
Chandra, G., Srivastava, S.N., 1972. J. Inorg. Nucl. Chem. 34, 197.
Chang, J.C., Garner, C.S., 1965. Inorg. Chem. 4, 209.
Chaudhary, K., Sharma, P.K., Banerji, K.K., 1999. Int. J. Chem. Kinet. 31, 469.
Cotton, F.A., Wilkinson, G., Murillo, C.A., Bochman, M., 1999. Advances in Inorganic Chemistry. Wiley-Intersci Publ, USA, p. 1229.
Das, A.K., 1996. J. Chem. Res. (synopsis) 4, 184.
Das, A.K., Das, M., 1995. Indian J. Chem. 34 (A), 866.
Das, C.M., Indrasenan, P., 1986. Ind. J. Chem. 25A, 605.
Das, C.M., Indrasenan, P., 1987. Ind. J. Chem. 26A, 717.
Das, A.K., Roy, A., Saha, B., Mohanty, R.K., Das, M., 2001. J. Phys. Org. Chem. 14, 333.
Day, J.C., Govindaraj, N., McBain, D.S., Skell, P.S., Tanko, J.M., 1986. J. Org. Chem. 51, 4959.
Domingos, A.P.J., Domingos, A.M.T.S., Gabral, J.M.P., 1969. J. Inorg. Nucl. Chem. 31, 2568.
Doty, T.E., Wannien, E., 1975. Food Technol. 11, 34.
Emis, E.S., 1966. Solvent Effect on Reaction Rates and Mechanism. Academic, NY.
Entelis, S.G., Tiger, R.P., 1976. Reaction Kinetics in the Liquid Phase. Wiley, New York.
Feigl, F., 1975. Spot Tests in Organic Analysis, seventh ed. Elsevier, NY.
Frost, A.A., Pearson, R.G., 1961. Kinetics and Mechanism, second ed. Wiley, NY.
Frost, A.A., Pearson, R.G., 1961. Kinetics and Mechanism, second ed. Wiley, New York.
Kantouch, A., Fattah, S.H.A., 1971. Chem. Zvest. 25, 222.
Katre, Y., Sharma, R., Joshi, G.K., Singh, A.K., 2012a. J. Disper. Sci. Technol. 33, 863.
Katre, Y., Mudliar, S.R., Joshi, G.K., Singh, A.K., 2012b. J. Disper.. Sci. Technol. 33, 1038.
Katre, Y., Tripathi, K., Singh, A.K., 2012c. J. Disper. Sci. Technol. 33, 447.
Katre, Y., Nayak, S., Sharma, D.N., Singh, A.K., 2012d. J. Disper. Sci. Technol. 38, 179.
Khanchandani, R., Sharma, P.K., Banerji, K.K., 1996. Ind. J. Chem. 35A, 57.
Khazaei, A., Manesh, A.A., 2005. J. Braz. Chem. Soc. 16, 874.
Kirsch, A., Luning, U., 1998. J. Prakt. Chem. 340, 129.
Kirsch, A., Luning, U., Kruger, O., 1999. J. Prakt. Chem. 341, 649.
Kong, F.Z., Tian, J.H., Jin, Z.L., 2002. Petrochem. Tech. 31, 387.
Kravtsov, V.I., Petrova, G.M., 1964. Russ. J. Inorg. Chem. (Engl Transl) 9, 552.
Krishnakumar, V., Balachandran, V., Chithambarathanu, T., 2005. Spectrochim. Acta 62, 918.
Kumbhat, V., Sharma, P.K., Banerjee, K.K., 2002. Int. J. Chem. Kinet. 34, 248.
Laidler, K.J., 1963. Reaction Kinetics. Pergamon Press, New York.
Laidler, K.J., Eyring, H., 1940. Ann. NY Acad. Sci. 39, 303.
Laidler, K.J., Landskroener, P.A., 1957. Trans. Faraday Soc. 52, 200.
Lyengar, T.A., Puttaswamy, D., Mahadevappa, S., 1990. Carbohydr. Res. 197, 119.
Malik, M.A., AL-Thabaiti, S.A., Khan, Z., 2009. Colloids Surf. A 337, 9.
Moelwyn-Hughes, E.A., 1961. Physical Chemistry, second ed. Pergamon Press, New York.
Moelwyn-Hughes, E.A., 1974. The Kinetics of Reaction in Solutions. Clarendon Press Oxford.
Mohanty, R.K., Das, M., Das, A.K., 1998. Indian J. Chem. 37 (A), 34.
Morris, J.C., Salazar, J.A., Wineman, M.A., 1948. Equilibrium studies on chloro compounds: the ionization constant of N-chloro-p-toluenesulfonamide. J. Am. Chem. Soc. 70, 2036.
Poulsen, I.A., Garner, C.S., 1962. J. Am. Chem. Soc. 84, 2032.
Ramachandrappa, R., Puttaswamy, G., Gowda, N.M.M., 1998. Int. J. Chem. Kinet. 30, 407.
Rao, V.S., Sethuram, B., Rao, T.N., 1979. Int. J. Chem. Kinet. 11, 165.
[a] Reddy, C.S., Kumar, T.V., 1995. Ind. J. Chem. 34A, 615[b]Kamble, D.L., Chougale, R.B., Nandibewoor, S.T., . Ind. J. Chem. 35A, 865.
Singh, A.K., Chopra, D., Rahmani, S., Singh, B., 1988. Carbohydr. Res. 314, 157.
Singh, A.K., Singh, V., Singh, A.K., Gupta, N., Singh, B., 2002. Carbohydr. Res. 337, 345.
Singh, A.K., Singh, V., Rahmani, S., Singh, A.K., Singh, B., 2003. J. Mol. Catal. A Chem. 197, 91.
Singh, A.K., Rahmani, S., Singh, B., Singh, R.K., Singh, M., 2004. J. Phys. Org. Chem. 17, 249.
Singh, A.K., Srivastava, J., Rahmani, S., Singh, V., 2006a. Carbohydr. Res. 341, 397.
Singh, A.K., Singh, V., Ashish, Srivastava J., 2006b. Ind. J. Chem. 45 (A), 599.
Singh, A.K., Srivastava, S., Srivastava, J., Singh, R., 2007a. Carbohydr. Res. 342, 1078.
Singh, A.K., Singh, R., Srivastava, J., Rehmani, R., Srivastava, S., 2007b. J. Organometal. Chem. 692, 4270.
Singh, S.P., Singh, A.K., Singh, A.K., 2008. J. Mol. Catal. A Chem. 293, 97.
Singh, A.K., Negi, R., Singh, S.P., Katre, Y., 2009. J. Mol. Catal. A Chem. 302, 36.
Singh, S.P., Singh, A.K., Singh, A.K., 2009a. J. Carbohydr. Chem. 28, 278.
Singh, A.K., Jain, B., Negi, R., Katre, Y.R., Singh, S.P., Sharma, V.K., 2009b. Catal. Lett. 131, 98.
Singh, A.K., Jain, B., Negi, R., Katre, Y.R., Singh, S.P., Sharma, V.K., 2009c. Trans. Met. Chem. 34, 521.
Singh, A.K., Negi, R., Katre, Y.R., 2009d. J. Mol. Catal. A Chem. 302, 36.

Singh, A.K., Sachdev, N., Srivastava, A., Jain, B., Katre, Y., 2012. Res. Chem. Intermed. 38, 507.
Taqui Khan, M.M., Chandraiah, G.R., Rao, A.P., 1986. Inorg. Chem. 25, 665.
Vogel, I., 1958. Elementary Practical Chemistry, Part III. Longmans-Green, London, p. 73.
Vyas, S., Sharma, P.K., 2001. Oxdn. Commun. 24, 248.
White, A., Handler, P., Smith, E.L., Stetten, D.W., 1959. Principle of Biochemistry, second ed. Mc-Graw-Hill, New York.
Zhai, Y.Q., Liu, H.M., Yang, L., Yang, G.Z., Song, W.Y., Liu, Y.K., 2007. Chem. Res. (Chinese) 23 (3), 333.